Deep-Sea Research II 71-76 (2012) 61–76

Contents lists available at SciVerse ScienceDirect

Deep-Sea Research II

journal homepage: www.elsevier.com/locate/dsr2

# Phytoplankton biomass and pigment responses to Fe amendments in the Pine Island and Amundsen polynyas

Matthew M. Mills [a,*], Anne-Carlijn Alderkamp [a,c], Charles-Edouard Thuróczy [b], Gert L. van Dijken [a], Patrick Laan [b], Hein J.W. de Baar [b,c], Kevin R. Arrigo [a]

[a] Department of Environmental Earth System Science, Stanford University, Stanford, CA 94305, USA
[b] Royal Netherlands Institute for Sea Research (Royal NIOZ), P.O. BOX 59, 1790 AB Den Burg, Texel, The Netherlands
[c] Department of Ocean Ecosystems, University of Groningen, Groningen, The Netherlands

ARTICLE INFO

Available online 16 March 2012

*Keywords:*
Phytoplankton
Fe
Ligand
Amundsen Polynya
Pine Island Polynya
*Phaeocystis antarctica*
Amundsen Sea

ABSTRACT

Nutrient addition experiments were performed during the austral summer in the Amundsen Sea (Southern Ocean) to investigate the availability of organically bound iron (Fe) to the phytoplankton communities, as well as assess their response to Fe amendment. Changes in autotrophic biomass, pigment concentration, maximum photochemical efficiency of photosystem II, and nutrient concentration were recorded in response to the addition of dissolved free Fe (DFe) and Fe bound to different model ligands. Analysis of pigment concentrations indicated that the autotrophic community was dominated by the prymnesiophyte *Phaeocystis antarctica* throughout most of the Amundsen Sea, although diatoms dominated in two experiments conducted in the marginal ice zone. Few significant differences in bulk community biomass (particulate organic carbon, nitrogen, and chlorophyll *a*) were observed, relative to the controls, in treatments with Fe added alone or bound to the ligand phytic acid. In contrast, when Fe was bound to the ligand desferrioxamine B (DFB), decreases in the bulk biomass indices were observed. The concentration of the diatom accessory pigment fucoxanthin showed little response to Fe additions, while the concentration of the *P. antarctica*-specific pigment, 19′-hexanoyloxyfucoxanthin (19′-hex), decreased when Fe was added alone or bound to the model ligands. Lastly, differences in the nitrate:phosphate ($NO_3^-$:$PO_4^{3-}$) utilization ratio were observed between the Fe-amended treatments, with Fe bound to DFB resulting in the lowest $NO_3^-$:$PO_4^{3-}$ uptake ratios (~10) and the remaining Fe treatments having higher $NO_3^-$:$PO_4^{3-}$ uptake ratios (~17). The data are discussed with respect to glacial inputs of Fe in the Amundsen Sea and the bioavailability of Fe. We suggest that the previously observed high $NO_3^-$:$PO_4^{3-}$ utilization ratio of *P. antarctica* is a consequence of its production of dissolved organic matter that acts as ligands and increases the bioavailability of Fe, thereby stimulating the uptake of $NO_3^-$.



## 1. Introduction

Phytoplankton primary productivity is generally constrained by the availability of either nutrients or light. In the case of nutrients, nitrogen is the primary limiting nutrient in most of the global ocean (Falkowski 1997). However, it is now well documented that in high nutrient low chlorophyll (HNLC) regions, which comprise approximately 30% of the global ocean area, the primary limiting nutrient is iron (Fe) (Martin and Fitzwater, 1988; Coale et al., 1996; Boyd et al., 2007). A low rate of Fe input and its low solubility in oxygenated seawater result in Fe concentrations sufficiently depleted to limit growth of the autotrophic community.

Fe is an integral part of the photosynthetic machinery and, as such, phytoplankton Fe demand is closely linked to the light environment (Sunda and Huntsman, 1997). Fe is a vital component of the reaction center proteins in both photosystems (PS) I and II, as well as the cytochrome $b_6f$ complex (Raven, 1990). Under low irradiance, more reaction centers are required to efficiently utilize the available light, thereby increasing phytoplankton Fe demand (Falkowski and Raven, 1997). Consequently, Fe and light can co-limit phytoplankton productivity in areas of the ocean where input of Fe is low, such as in HNLC regions (De Baar et al., 2005).

Additionally, Fe is critical to the uptake and utilization by phytoplankton of several nitrogenous compounds. The enzymes nitrate reductase and nitrite reductase contain Fe co-factors. Both field and laboratory experiments have shown that $NO_3^-$ drawdown is greater when Fe-limitation is relieved (Berg et al., 2011).

* Corresponding author.
*E-mail address:* mmmills@stanford.edu (M.M. Mills).

0967-0645/$ - see front matter © 2012 Elsevier Ltd. All rights reserved.
http://dx.doi.org/10.1016/j.dsr2.2012.03.008

However, it has also been suggested that, rather than $NO_3^-$ reduction being inhibited when Fe is limiting, the reduction of $NO_2^-$ to $NH_4^+$ is impaired (Milligan and Harrison, 2000). In addition, the nitrogenase enzyme that catalyzes the fixation of $N_2$ to $NH_4^+$ has a high Fe requirement, and rates of $N_2$ fixation have been correlated to oceanic Fe concentrations (Voss et al., 2004; Moore et al., 2009). High rates of autotrophic production, therefore, depend on there being sufficient Fe to meet phytoplankton demands.

Fe availability to phytoplankton is determined by several factors that include chemical speciation, photochemistry, and biological processes. In seawater, Fe is operationally separated into different phases that include soluble, dissolved, particulate, and reactive (Wong et al., 2006). Fe in the particulate fraction is primarily found as mineral Fe-oxyhydroxides, biologically associated, or adsorbed to particles. In the dissolved fraction, the majority ($>99.9\%$) of Fe is bound to organic matter (ligands) that keep Fe dissolved in seawater (Rue and Bruland, 1997). Fe-binding ligands are primarily biogenic (e.g. siderophores, porphyrins, and organic exudates) or humic in nature and may be either strongly or weakly binding. The stronger Fe-binding ligands ($L_1$) are primarily found in the surface ocean and are believed to be siderophores produced by bacteria (Boyd and Ellwood, 2010). The weaker Fe-binding ligands ($L_2$) are less abundant than $L_1$ and are believed to be either formed from the decay of organic matter or released during grazing (Boyd and Ellwood, 2010). Saccharides produced during phytoplankton exudation, viral lysis of cells, and zooplankton grazing are weak Fe-binding ligands (Hassler et al., 2009, 2011) and are the dominant constituent of the colloidal size fraction of the dissolved organic matter pool in the ocean (Benner, 2011). Despite their weaker binding strength, their high concentration makes them potentially significant components of the Fe cycle and, therefore, they may contribute to the control of phytoplankton productivity in the ocean.

The Southern ocean is the largest of the world's HNLC regions. It is also one of the most important oceanic areas for the biological uptake and sequestration of atmospheric $CO_2$ (Takahashi et al., 2002). Of the roughly 20 Gt of atmospheric $CO_2$ that is taken up annually by the Southern Ocean, approximately half is mediated by the activity of phytoplankton (Takahashi et al., 2002; Roy et al., 2003; Gurney et al., 2004). The continental shelves are one of the most productive regions, accounting for almost 30% of annual production in the Southern Ocean (Arrigo et al., 1998). The majority of this high productivity is found within the polynyas (areas of open water located in waters that would be expected to be ice covered) that surround the Antarctic continent. Although they are typically the first sites to be exposed to the increasing springtime irradiance, these highly productive polynyas can become Fe-limited, with approximately 30% of the initial macronutrient inventory left unutilized at the end of the spring/summer phytoplankton bloom (Sedwick et al., 2000; Tagliabue and Arrigo, 2005).

In the Amundsen Polynya (AP) and the Pine Island Polynya (PIP), located along the western Antarctic shelf, chlorophyll *a* (Chl *a*) concentrations and autotrophic productivity are among the highest of all the polynyas surrounding Antarctica. Springtime concentrations of Chl *a* regularly surpass 10 mg $m^{-3}$ (Arrigo and van Dijken, 2003). Recently, much interest has centered on the western Antarctic shelf as a result of the rapidly accelerating glacial melt in this region, including the Pine Island, Thwaites, Dotson, and Getz glaciers, all of which border either the PIP or the AP. Circumpolar deep water (CDW) that flows onto and across the continental shelf in this region is presumed to mix with subglacial melt waters, increasing their temperatures and melting the glaciers from below. This results in buoyancy-driven upwelling of nutrient-rich meltwater modified CDW (meltwater MCDW) at the glacier face (Gerringa et al., 2012). The input of nutrients and/or Fe from the glaciers are as of yet not well understood, but this upwelling potentially drives the high Chl *a* concentrations and phytoplankton productivity observed in these polynyas (Alderkamp et al., 2012).

Here we report the results of nutrient addition bioassays conducted in the PIP and AP during austral summer of 2009. The primary objective of the experiments was to assess the availability of organically bound Fe to the phytoplankton population and understand their response to Fe amendment. We measured the changes in autotrophic biomass, pigments, and photosynthetic efficiency in response to amendments of dissolved free Fe or Fe bound to different model ligands.

## 2. Methods

### 2.1. Sampling locations

Between 13 January and 18 February 2009, 11 bioassay experiments were carried out in the Southern Ocean in and around the Amundsen Sea (66.9°S–75.1°S, 103°W–128°W, Fig. 1). The experiments were grouped using spatial and physical criteria such as proximity to the ice shelf, sea ice concentration on the day of water collection, and temperature and salinity of the sampling stations (Table 1, Fig. 2). Temperature and salinity were measured at each experimental site using a conductivity, temperature, and depth sensor (CTD, SBE 9/11+, Sea-Bird Electronics, Inc., Washington, USA) attached to a rosette. Sea ice concentration was determined using AMSR-E satellite imagery. Four station types were defined; open ocean, marginal ice zone (MIZ), polynya, and Pine Island Bay (PIB). One experiment (Exp. 12) was conducted north of the continental shelf at a water depth $>4000$ m and represents the open ocean station (Fig. 1). The remaining stations were all in shallower waters ranging from $\sim$300 to 1100 m. The MIZ stations (Exps. 1, 2, 9, 11) were defined as those where sea ice concentration on the day of sampling exceeded 15% (Table 1) and exhibited the lowest surface temperatures ($<-1.5$ °C, Fig. 3). The PIB stations (Exps. 3, 4, 5) were in open water within the PIP but located close to the ice shelf edge. These stations had the highest temperature (0.46–0.65 °C) and salinity ($\sim$34). Finally, the polynya stations were in open water ($<15\%$ ice cover) further offshore within either the PIP or the AP (Exps. 6, 7, 8).

### 2.2. Bioassay experiments

Surface seawater was collected from a depth of 10 m using six trace metal clean GO-FLO bottles (General Oceanics, Inc.) attached to a trace metal clean rosette on a non-metal wire. Once on deck, the bottles were transported to a trace metal clean container (Class 1000) where they were immediately sampled using an acid cleaned PTFE tube extending into a clean laminar flow bench for initial macronutrient ($NO_3^-$ and $PO_4^{3-}$), dissolved iron (DFe), and total dissolvable iron (TDFe) concentrations. Samples for Fe speciation measurements were taken this way as well. Initial waters were additionally sampled for Chl *a* concentration, maximum photochemical efficiency of PS II ($F_v$:$F_m$), particulate organic carbon (POC), particulate organic nitrogen (PON), and pigment complement by HPLC analysis.

Water from the GO-FLO bottles was then dispensed into randomly selected 1.18 L acid washed polycarbonate bottles through acid cleaned silicone tubing. The bottles were sealed and then transported to a trace metal clean bubble (Class 1000) where all further manipulations took place. Under a laminar flow bench (Class 100), Fe and ligands were added alone or in combination to achieve a final concentration of 4 nmol $L^{-1}$. When added together, the Fe and ligands were premixed in a 1:1 M ratio. Fe+ligand stocks were mixed in room temperature milli-Q water $>24$ h prior

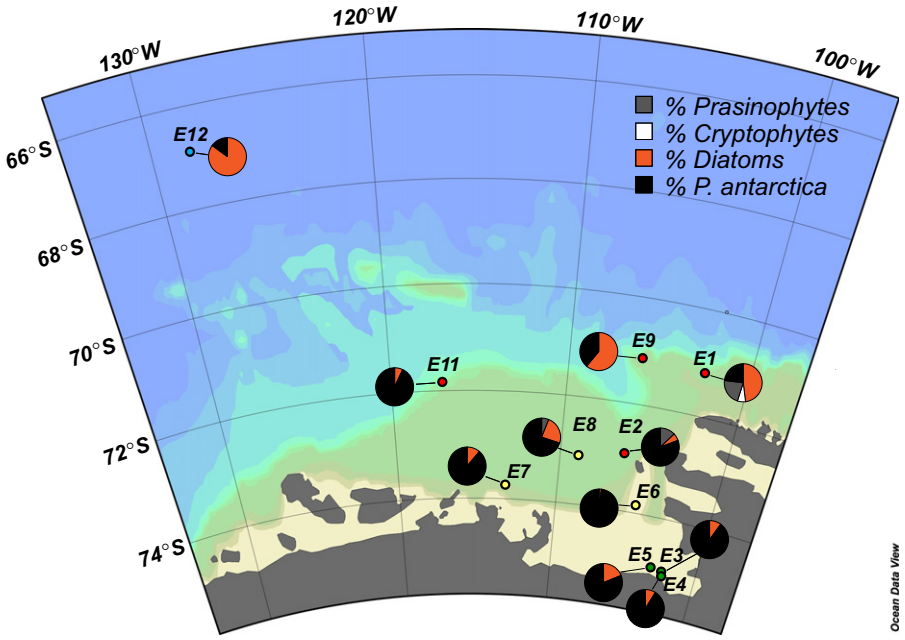


**Fig. 1.** Map showing the location of the bioassay experiments conducted during the NBP0901 cruise in the Amundsen Sea. The experimental sites are color coded according to the experimental type; blue: open ocean experiment, red: MIZ experiment, yellow: polynya experiment, and green: PIB experiment. The initial percent composition of the phytoplankton community is shown next to each site.

**Table 1**
Initial conditions for bioassay experiments. Numbers in ( ) represent standard error of the mean. The mean ± (SE) of a individual sample analyzed four times is presented for DFe, TDFe, Lt, and Log $K'$.

| Latitude (°S)<br>Longitude (°W) | 71.2,<br>102.4 | 73.0,<br>106.4 | 75.0,<br>102.0 | 75.1,<br>102.0 | 75.1,<br>102.0 | 75.0,<br>102.7 | 73.9,<br>105.0 | 73.7,<br>113.3 | 71.2,<br>102.4 | 71.9,<br>118.7 | 66.9,<br>128.9 |
|---|---|---|---|---|---|---|---|---|---|---|---|
| Experiment | 1 | 2 | 3 | 4 | 5 | 6 | 7 | 8 | 9 | 11 | 12 |
| Ice concentration (%) | 89 | 56 | 0 | 0 | 0 | 0 | 0 | 7 | 78 | 83 | 0 |
| Chl a (mg $m^{-3}$) | 0.7 | 8.0 (0.66) | 4.9 (0.24) | 3.2 (0.63) | 4.3 (0.44) | 7.7 (0.92) | 4.4 (0.72) | 3.6 (0.42) | 1.2 (0.19) | 2.9 (0.38) | 0.29 (0.11) |
| $F_v$:$F_m$ | 0.57 | 0.47 | 0.46 | 0.49 | 0.45 | 0.34 | 0.49 | 0.48 | 0.39 | 0.49 | 0.29 |
| Fucoxanthin (mg $m^{-3}$) | 0.3 | 1.2 (0.05) | 0.5 (0.01) | 0.39 (0.02) | 0.6 (0.11) | 0.6 (0.05) | 0.9 (0.10) | 0.8 (0.05) | 0.6 (0.01) | 0.5 (0.02) | 0.2 (0.01) |
| 19′-Hexanoyloxy-fucoxanthin (mg $m^{-3}$) | 0.1 | 5.8 (0.34) | 3.5 (0.06) | 2.3 (0.20) | 3.0 (0.08) | 7.1 (0.49) | 2.9 (0.39) | 2.1 (0.05) | 0.3 (0.01) | 2.4 (0.12) | 0.04 (0.002) |
| $NO_3^-$ (mmol $m^{-3}$) | 24.42 | 16.1 | 10.7 | 12.5 | 9.0 | 3.5 | 2.7 | ND | ND | 16.1 | 23.7 |
| $PO_4^{3-}$ (mmol $m^{-3}$) | 1.4 | 1.2 | 1.0 | 1.2 | 1.0 | 0.7 | 0.5 | ND | ND | 1.0 | 1.5 |
| POC (mmol $m^{-3}$) | 8.7 | 47.8 | 48.3 | 32.4 | 44.3 | 64.4 | 51.6 | 35.1 | 14.7 | 43.4 | 14.9 |
| PON (mmol $m^{-3}$) | 1.2 | 7.6 | 7.9 | 4.8 | 6.0 | 9.7 | 8.3 | 6.3 | 3.0 | 6.5 | 1.7 |
| DFe (μmol $m^{-3}$) | 0.22 (0.025) | 0.10 (0.010) | 0.21 (0.017) | 0.25 (0.008) | 0.09 (0.001) | 0.09 (0.018) | 0.11 (0.010) | 0.08 (0.005) | 0.13 (0.006) | 0.09 (0.007) | 0.10 (0.027) |
| TDFe (μmol $m^{-3}$) | 1.42 (0.018) | 3.47 (0.018) | 8.69 (0.088) | 8.54 (0.048) | 6.46 (0.015) | 1.27 (0.015) | 2.98 (0.006) | 3.59 (0.037) | 1.59 (0.019) | 3.55 (0.012) | 1.43 (0.064) |
| Lt (nEq of M Fe) | 0.52 (0.270) | 0.37 (0.186) | 0.64 (0.096) | 0.73 (0.148) | 0.62 (0.173) | 0.22 (0.262) | 1.13 (0.174) | 0.91 (0.092) | 0.85 (0.039) | 0.91 (0.051) | ND |
| Excess $L'$ (nEq of M Fe) | 0.30 | 0.30 | 0.40 | 0.29 | 0.53 | 0.13 | 1.02 | 0.83 | 0.73 | 0.82 | ND |
| Log $K'$ ($mol^{-1}$) | 21.44 (0.32) | 21.50 (0.32) | 22.12 (0.41) | 21.60 (0.21) | 21.53 (0.23) | 21.53 (0.23) | 21.84 (0.22) | 21.90 (0.15) | 22.31 (0.12) | 22.16 (0.11) | ND |

ND: No data

to the start of experiments and then stored in a refrigerator (4 °C). We used desferrioxamine B (DFB) and phytic acid (PA) as model ligands (Maldonado et al., 2005). Fe bound to either of the model ligands was determined to be photo-stable in artificial seawater and natural sunlight experiments (Maldonado et al., 2005).

The experimental treatments included a control (C), +Fe, +DFB, +PA, +DFB+Fe, and +PA+Fe, all conducted in triplicate. Once filled, the bottles were tightly capped, the neck of each bottle wrapped with parafilm, and the bottles placed in Ziploc bags prior to being placed in on-deck incubators with circulating surface seawater for 4–5 day before the final samples were collected. Light in the incubators was attenuated to 25% of incident irradiance using window screen.

All treatments were sampled for the macronutrients $NO_3^-$ and $PO_4^{3-}$, $F_v$:$F_m$, POC, PON, and Chl *a* concentration and pigment complement by HPLC analysis at the end of the incubation period.

### 2.3. Analytical methods

Samples for fluorometric analysis of Chl *a* were filtered onto 25 mm Whatman GF/F filters (nominal pore size 0.7 μm) placed in 5 mL of 90% acetone, and extracted in the dark at 3 °C for 24 h.

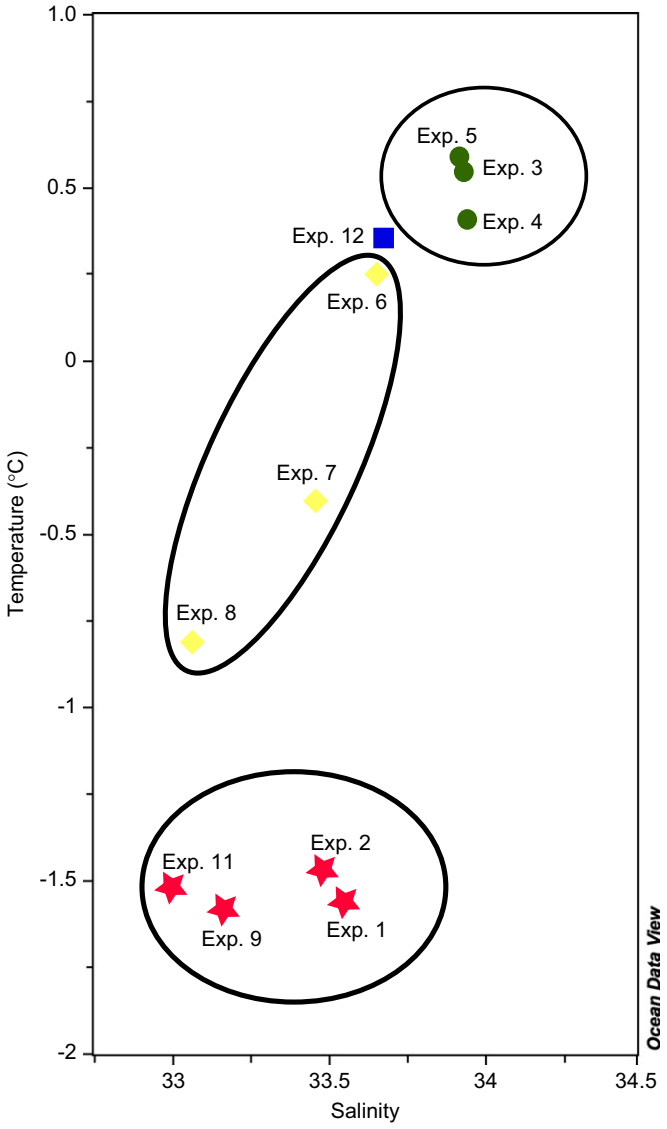


**Fig. 2.** Salinity and temperature of the waters used to initiate each experiment. Experiments were grouped using these temperature and salinity relationships, as well as ice concentration at each site on the day of sampling. Colors represent experiment type as shown in Fig. 1.

Chl *a* was measured fluorometrically (Holm-Hansen et al., 1965) using a Turner Fluorometer 10-AU (Turner Designs, Inc.) The bulk $F_v$:$F_m$ of the phytoplankton community was measured on dark acclimated (30 min.) aliquots of initial and treatment waters using a WATER-PAM (Walz, GmbH, Germany). The WATER-PAM was blanked using filtered experimental water prior to analyzing samples. POC and PON samples were collected by filtering subsamples onto pre-combusted (450 °C for 4 h) 25 mm Whatman GF/F filters. The filters were then immediately frozen and stored at -20 °C. Prior to analysis, the samples were fumed with concentrated HCl, dried at 60 °C, and packed into tin capsules (Costech Analytical Technologies, Inc.) for elemental analysis on Carlo-Erba NA-1500 elemental analyzer. Acetanilide was used as a calibration standard. Samples for phytoplankton pigment composition and concentration were collected and immediately filtered through GF/F filters (Whatman), flash frozen in liquid nitrogen, and stored at −80 °C until HPLC analysis. Details of the HPLC method and the subsequent CHEMTAX analysis are described in Alderkamp et al. (2012).

The initial samples for DFe and TDFe analyses were filtered (0.2 μm), acidified (pH=1.8 by adding 2 ml per liter of ultraclean 12 M HCl (Baseline® Hydrochloric Acid, Seastar Chemicals), and then measured directly on board by automated Flow Injection Analysis (FIA) using the modified method of De Jong et al. (1998) as described in De Baar et al. (2008). Organic complexation of Fe in the initial waters was investigated using Competing Ligand Exchange-Adsorptive Stripping Voltammetry (CLE-AdSV) using 2-(2-Thiazolylazo)-p-cresol (TAC) as a competing ligand (Croot and Johanson, 2000). Further details of the DFe, and TDFe analyses, as well as the ligand measurements can be found in Gerringa et al. (2012) and Thuróczy et al. (2012).

Samples for $NO_3^-$ and $PO_4^{3-}$ analysis from initial and treatment waters were filtered through acid rinsed GF/F filters and collected into acid washed polystyrene vials (E&K Scientific). The samples were immediately frozen (−20 °C) until analysis on a SmartChem™ 200 discrete analyzer (Westco Scientific Instruments, Inc.) using standard colorimetric protocols (Grasshoff et al., 1999). Additional samples for DFe, TDFe, ligand concentration (Lt), ligand binding strength, and excess ligand concentration ($L'$) were sampled from all initial waters. The methods used in the collection and analyses of these samples are described in Gerringa et al. (2012) and Thuróczy et al. (2012).

Finally, statistical analyses were performed to determine differences between control and treatment means using a one-way analysis of variance (ANOVA) followed by a Fisher-PLSD means comparison test. Regression analysis was also used to assess differences between responses in Fe amended treatments. Differences between slopes of the regressions were detected using a *t*-test.

## 3. Results

### 3.1. Initial conditions

The initial concentration of Chl *a* in waters used for experiments increased southward from 0.3 mg $m^{-3}$ at the open ocean site to a peak of ~7 mg $m^{-3}$ at sites in the center of the PIP (Table 1). At the face of Pine Island Glacier (PIG), concentrations of Chl *a* were lower (3–5 mg $m^{-3}$) than in the center of the polynya. The photochemical efficiency of PS II ($F_v$:$F_m$) was lowest at the open ocean station (0.29) and varied from 0.30 to 0.57 in no consistent manner at the other experimental sites. The accessory pigments fucoxanthin (fuco), a marker pigment of diatoms, and 19′-hexanoyloxyfucoxanthin (19′-hex), indicative of haptophytes, followed a distribution similar to that of Chl *a*. Concentrations of 19′-hex (0.04–7.1 mg $m^{-3}$) were greater than fuco (0.2–1.2 mg $m^{-3}$) at all but the three most northern experimental sites (Exp. 1, 9 and 12, Table 1). Chemtax analysis of pigment composition indicated that 70–98% of total Chl *a* concentration was attributable to the haptophyte *P. antarctica* at all experimental stations within the polynya, as well as at two of the four MIZ stations (Fig. 1). Diatoms (2–24%), prasinophytes (0–13%), and cryptophytes (<10%) accounted for a smaller fraction of the community at these stations. Of the two MIZ stations that had relatively low *P. antarctica* abundance, diatoms (45–62%) dominated the Chl *a* signal. At the open ocean station, the primary contributors to the Chl *a* pigment pool were diatoms (85%) and *P. antarctica* (~15%).

Initial $NO_3^-$ concentrations were above the level of detection at all stations where data were collected, ranging from ~24 mmol $m^{-3}$ at the two experimental stations with the lowest Chl *a* concentrations (Exp. 1 and Exp. 12) to ~3 mmol $m^{-3}$ at the polynya stations where Exp. 6 and Exp. 7 were conducted (Table 1, no initial nutrient data were collected for Exps. 8 and 9). Phosphate ($PO_4^{3-}$) concentrations exhibited a similar spatial pattern (Table 1). The ratio of $NO_3^-$ to $PO_4^{3-}$ in Southern Ocean waters is

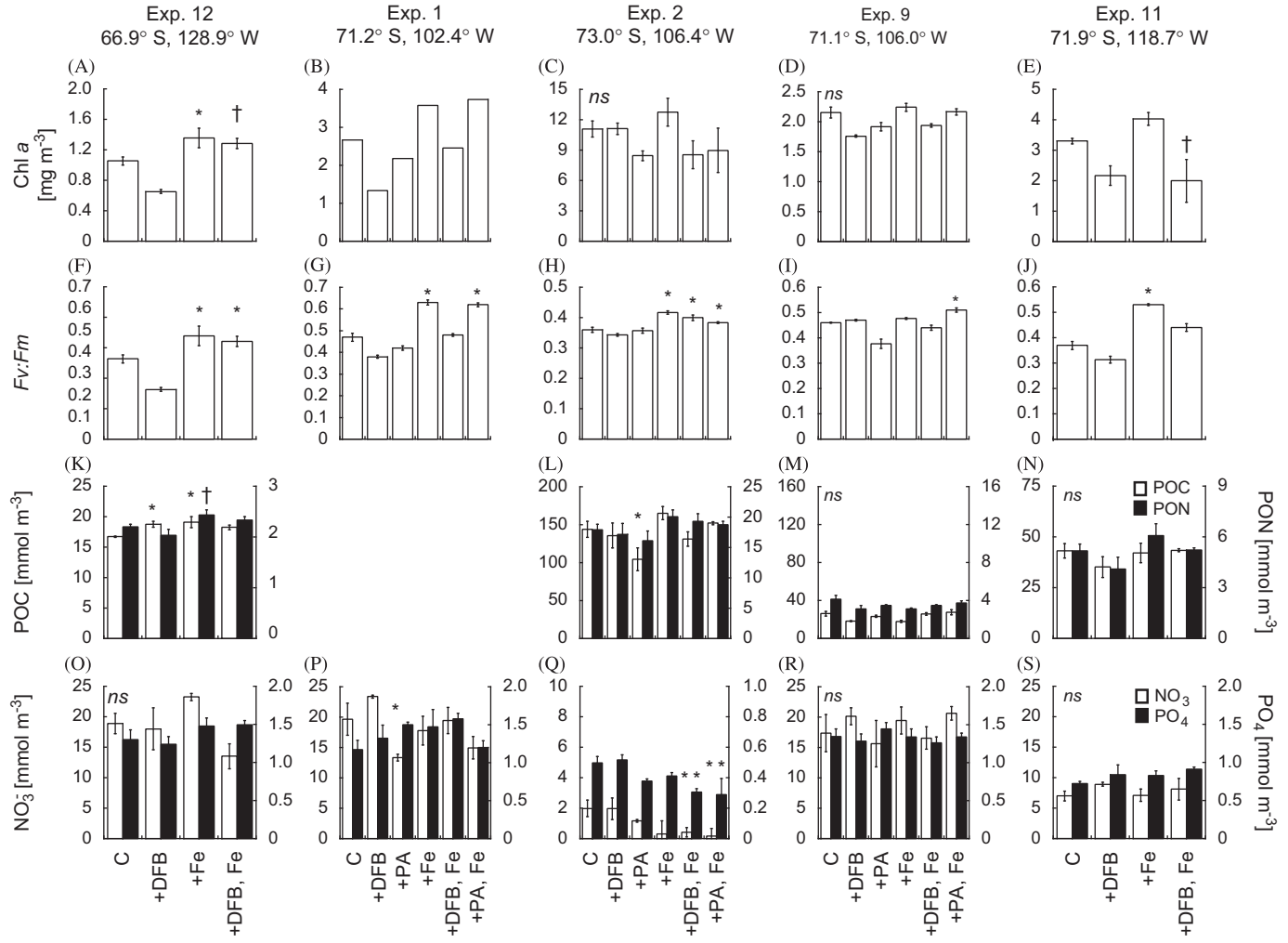


**Fig. 3.** Comparison of (A–E) Chl *a* concentration, (F–J) $F_v$:$F_m$, (K–N) POC and PON concentrations, (O–S) and $NO_3^-$ and $PO_4^{3-}$ concentration in the different Fe and ligand treatments from the open ocean (Exp. 12) and the MIZ (Exps. 1, 2, 9, 11) experiments. Error bars represent ± 1 standard error. Asterisks (*) and crosses (†) indicate significant difference from the control at the $\alpha = 0.05$ and 0.07 significance levels, respectively. *ns* indicates no significant differences between the control and treatments.

strongly linked to the composition of the phytoplankton community, with waters dominated by diatoms having low $NO_3^-$:$PO_4^{3-}$ uptake ratios, and waters dominated by *P. antarctica* having high $NO_3^-$:$PO_4^{3-}$ uptake ratios, relative to Redfield proportions (Arrigo et al., 1999). Consistent with this, at the stations south of 71°S, where initial nutrient data are available, the $NO_3^-$:$PO_4^{3-}$ ratios of the initial waters varied between 5 and 13. At stations north of 71°S, $NO_3^-$:$PO_4^{3-}$ ratios were substantially higher (15.8–17.4), though similar to the Redfield ratio (16). The $NO_3^-$:$PO_4^{3-}$ ratio of initial waters was negatively correlated to Chl *a* concentrations ($r = -0.67$, $p < 0.05$) across all experimental stations. Assuming that the $NO_3^-$:$PO_4^{3-}$ ratios of the initial experimental waters represented the residual ratio after phytoplankton nutrient consumption, the uptake ratio for the phytoplankton communities blooming in the region can be calculated by regressing $NO_3^-$ concentrations against $PO_4^{3-}$ concentrations for all initial waters. The resulting slope is 22 ± 3.4, indicating that the $NO_3^-$:$PO_4^{3-}$ consumption ratio of the blooming phytoplankton in the AP and the PIP was greater than Redfield proportions, consistent with uptake by *P. antarctica*.

Initial concentrations of total dissolvable Fe (TDFe) were highest at the stations located close to the face of the PIG, measuring 6.5–8.7 μmol $m^{-3}$, while at the remaining experimental sites, TDFe ranged from 1.3–3.6 μmol $m^{-3}$. Likewise, dissolved Fe (DFe) concentrations were high close to the PIG (0.21–0.25 μmol $m^{-3}$), with concentrations of < 0.13 μmol $m^3$ at most of the remaining sites where experiments were conducted. In the initial waters for Exp. 5 in PIB, anomalously low initial DFe concentrations (0.09 μmol $m^{-3}$) were detected, while the initial waters for Exp. 1 in the MIZ had relatively high DFe concentrations (0.22 μmol $m^{-3}$) (Table 1). Although initial ligand concentrations at the experimental sites showed no apparent spatial pattern within the PIP, a larger analysis of ligand concentrations in the Amundsen Sea document an increase in ligand content along a transect that extends northwestward away from the PIG and into the PIP (Thuróczy et al., 2012). The highest ligand concentration in the experimental sites was observed in the AP at Exp. 7 (1.13 nEq of M Fe), while the lowest concentration (0.22 nEq of M Fe) was measured in the center of the PIP at Exp. 6. The concentration of excess ligands ranged from 0.29–1.02 [nEq of M Fe] and was highest in the AP (Exp 7) and lowest in the PIP (Exp 6). Finally, ligand binding strength (Log $K'$ [$mol^{-1}$] at experimental stations showed little variation between the polynyas (21.7 ± 0.24 nEq of M Fe), PIB (21.8 ± 0.32 nEq of M Fe), or the MIZ (22.0 ± 0.36 nEq of M Fe).

### 3.2. Bulk community response to nutrient additions

#### 3.2.1. Open ocean

In the open ocean experiment (Exp. 12), Chl *a* concentration in the +Fe treatment was a 1.4–fold higher than the control by the end of the four-day incubation (Fig. 3A). However, the +DFB+Fe treatment showed no significant Chl *a* increase. $F_v$:$F_m$ increased

significantly (1.18–1.26-fold) in both of the Fe-amended treatments (Fig. 3F). Biomass increased significantly in this experiment, although not in all Fe treatments (Fig. 3K). The POC concentration increased 1.14-fold in the +Fe treatment without a corresponding increase in PON. Additionally, POC increased slightly (+9%), although significantly, in the +DFB treatment. Finally, no significant changes in $NO_3^-$ or $PO_4^{3-}$ concentrations were detected as a result of Fe additions (Fig. 3O). These changes suggest that the phytoplankton community in the open ocean was Fe-limited.

### 3.2.2. MIZ

Addition of Fe at the MIZ stations resulted in increased Chl *a* in Exp. 1 (Fig. 3B) but not in Exps. 2, 9, or 11 (Fig. 3C–E). In Exp. 1, the addition of Fe bound to the model ligand PA stimulated an increase in Chl *a*. Likewise, $F_v$:$F_m$ was stimulated in this experiment (Fig. 3G), as well as in all the Fe treatments in Exp. 2 (Fig. 3H), the +PA+Fe treatment in Exp. 9 (Fig. 3I), and the +Fe treatment in Exp 11 (Fig. 4J). Chl *a* and $F_v$:$F_m$ were unchanged or reduced in the +DFB+Fe treatments in all MIZ experiments, except in Exp. 2 where $F_v$:$F_m$ was increased above the control in the +DFB+Fe treatment (Fig. 3B–E and G–J). Furthermore, in the majority of MIZ experiments, no significant biomass (POC or PON) increases (Fig. 3L–N) or changes in macronutrient ($NO_3^-$ or $PO_4^{3-}$, Fig. 3P–S) concentrations were detected in response to the addition of Fe in any form. However, there was some evidence of a response to Fe additions. For example, $NO_3^-$ concentration declined by ~6 μmol $L^{-1}$ over the 4 day experiment in the +PA treatment of Exp. 1 (Fig. 3P). A lack of POC and PON samples in

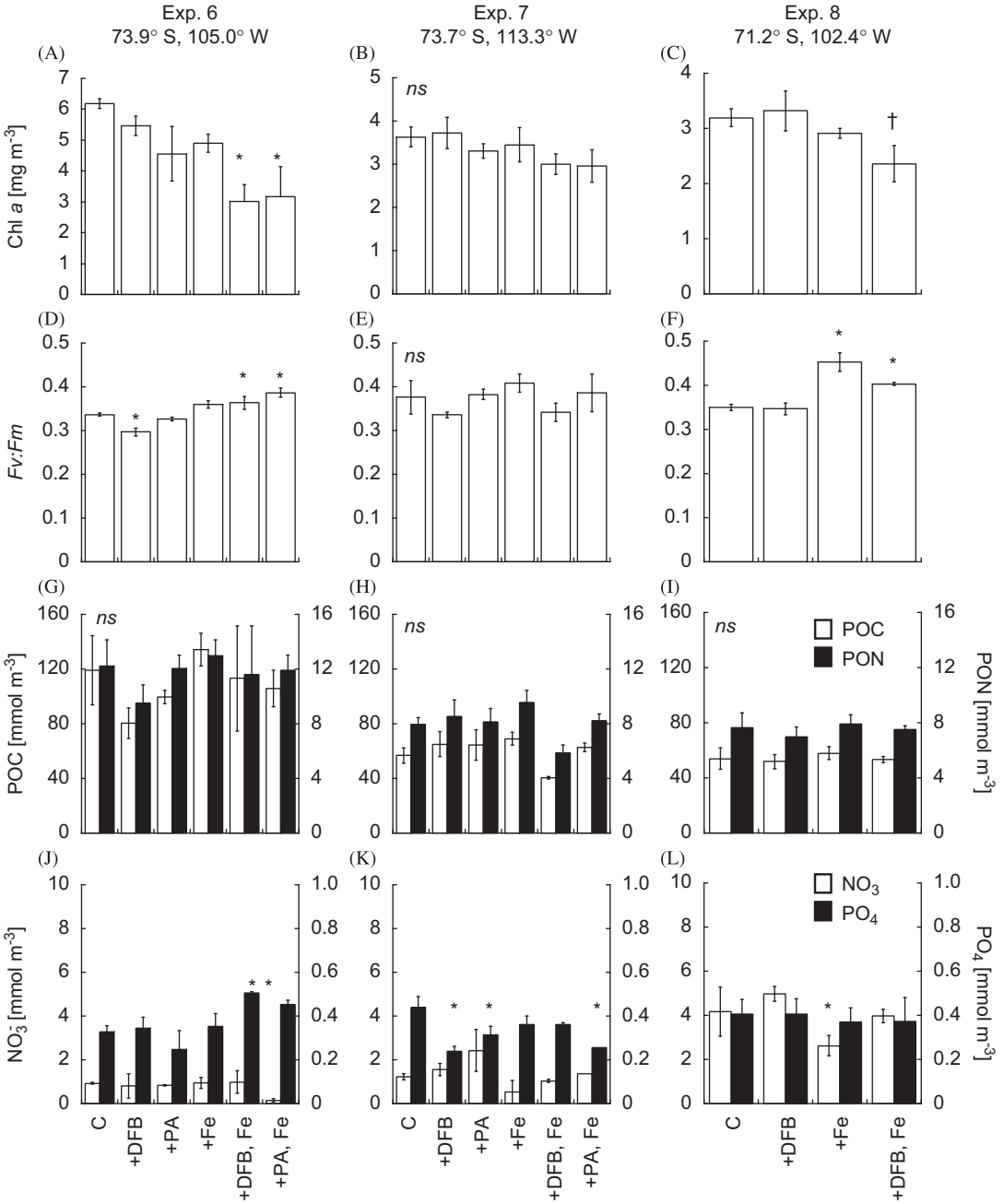


**Fig. 4.** Comparison of (A–C) Chl *a* concentration, (D–F) $F_v$:$F_m$, (G–I) POC and PON concentration, (J–L) and $NO_3^-$ and $PO_4^{3-}$ concentration in the different treatments from the polynya experiments (Exps. 6, 7, 8). Error bars represent ± 1 standard error. Asterisks (*) and crosses (†) indicate significant difference from the control at the $\alpha = 0.05$ and 0.07 significance levels, respectively. *ns* indicates no significant differences between the control and treatments.

this experiment prevented us from determining if this decrease was accompanied by a stoichiometric increase in C or N biomass. In Exp. 2, POC decreased in the +PA treatment (Fig. 3L) while the ligand+Fe treatments for this experiment had lower macronutrient concentrations relative to the control (Fig. 3Q). Beyond the enhanced (relative to the control) $F_v$:$F_m$ in the +Fe and the +PA+Fe treatment, there were few consistent bulk community responses in the experiments conducted at the MIZ sites.

### 3.2.3. Polynyas

In contrast to the open ocean station, but similar to most of the MIZ stations, the polynya experiments (Exps. 6–8) showed no appreciable increase in Chl *a* concentration in response to the Fe amendments over the 4–5 day incubation (Fig. 4A–C). In fact, significant decreases of 0.25–0.5-fold, relative to controls, were detected in two of the three polynya experiments (Fig. 4A and C). Despite the lack of a positive Chl *a* response in the polynya experiments, $F_v$:$F_m$ increased in response to the +Fe amendment in Exp. 8 (Fig. 4D) and to the ligand-bound Fe amendments in both Exps. 6 and 8 (Fig. 4D and F). No $F_v$:$F_m$ response was observed in Exp. 7 (Fig. 4E). Concentrations of POC and PON also remained unchanged relative to the control in the polynya experiments (Fig. 4G–I). Although some significant macronutrient changes relative to controls were detected in some polynya experiments (Fig. 4J–L), no obvious pattern was observed. For example, $NO_3^-$ concentrations were lower in the +Fe treatment of Exp. 8 (Fig. 4L) but not in the other +DFB+Fe treatment. Additionally, $PO_4^{3-}$ was lower relative to the control only in the +DFB, +PA, and +PA+Fe treatments of Exp. 7 (Fig. 4K). The general observation of increased $F_v$:$F_m$, as well as the increased consumption of $NO_3^-$ and $PO_4^{3-}$ in Exps. 6 and 8, respectively, upon exposure to increased Fe concentrations at the polynya stations indicates some level of Fe stress. However, the lack of consistent increases in Chl *a*, POC, and PON, in combination with the relatively high $F_v$:$F_m$ values, suggests that the bulk community was not strongly Fe-limited and that there was appreciable bioavailable Fe in initial experimental source waters.

### 3.2.4. Pine Island Bay

At the three PIB stations (Exp. 3–5), a positive Chl *a* response was detected only in Exp. 5 (Fig. 5C), in which the +PA, and the +PA+Fe amended treatments increased ~1.5-fold. In this same experiment, $F_v$:$F_m$ increased in the Fe-amended treatments, whereas the ligand-only additions showed no $F_v$:$F_m$ increase (Fig. 5F). In Exps. 3 and 4, the +Fe and +PA+Fe treatments elicited $F_v$:$F_m$ responses that were higher than controls while the +DFB+Fe additions resulted in no significant $F_v$:$F_m$ increase (Fig. 5D–F). Furthermore, the ligand-only amendments in Exp. 3 resulted in decreased $F_v$:$F_m$ (Fig. 5D). These positive Chl *a* and $F_v$:$F_m$ changes in response to Fe or ligand-bound Fe at the PIB stations coincided with increased POC and/or PON concentrations in Exps. 3 and 4, but only in the +PA+Fe (Fig. 5G and H) treatments. No significant changes in POC or PON concentrations were detected in Exp. 5 (Fig. 5I). Lastly, macronutrient concentrations were reduced below controls only in the +PA+Fe treatment of Exp. 3; the final $NO_3^-$ and $PO_4^{3-}$ were 10–20% of that in the controls (Fig. 5J).

### 3.2.5. Bulk community $NO_3^-$ vs. $PO_4^{3-}$ uptake

An analysis of the $NO_3^-$:$PO_4^{3-}$ ratio of the treatments at the end of the experiments compared to the initial starting waters provides an estimate of the relative uptake of $NO_3^-$ vs. $PO_4^{3-}$ and its relation to Fe availability in the Amundsen Sea. We averaged $NO_3^-$:$PO_4^{3-}$ ratios from the same treatments at the different station types (i.e. open ocean, MIZ, polynya, and PIB). $NO_3^-$:$PO_4^{3-}$ ratios of initial waters were not available for all experiments (e.g. Exps. 8 and 9); therefore, these experiments were not included in the analysis.

The initial waters of the open ocean and MIZ experiments had $NO_3^-$:$PO_4^{3-}$ ratios that averaged $\sim 16 \pm 0.6$, equal to the Redfield ratio. In the experimental waters from the polynyas and PIB, the $NO_3^-$:$PO_4^{3-}$ ratios were significantly lower than Redfield proportions, averaging $5 \pm 0.1$ and $10 \pm 0.7$, respectively. Changes in the $NO_3^-$:$PO_4^{3-}$ ratio during the experiments indicate consumption of $NO_3^-$ and $PO_4^{3-}$ that is different from the starting ratio.

The control waters from the open ocean and PIB experiments showed little change in the $NO_3^-$:$PO_4^{3-}$ ratio relative to initial values (Fig. 6A and D). This was not the case in the MIZ and polynya experiments, in which the controls had lower $NO_3^-$:$PO_4^{3-}$ ratios than the initial starting waters (Fig. 6B and C). The ligand-only additions had little effect on $NO_3^-$:$PO_4^{3-}$ ratios except in the PIB experiments where the +PA amendment resulted in lower $NO_3^-$:$PO_4^{3-}$ ratios. In the open ocean experiment (Exp. 12), there was no detectable change in the $NO_3^-$:$PO_4^{3-}$ ratio in most treatments relative to the initial waters (Fig. 6A). The only exception was in the +DFB+Fe treatment in which the $NO_3^-$:$PO_4^{3-}$ was reduced by 43%. In contrast, the $NO_3^-$:$PO_4^{3-}$ ratio in the Fe amended treatments in the MIZ and Polynya experiments were lower than their respective initial waters (Fig. 6B and C). There was a similar response in the PIB experiments for the +Fe and +PA+Fe treatments; however, the +DFB+Fe treatment actually had a higher $NO_3^-$:$PO_4^{3-}$ ratio than the initial (Fig. 6D).

We also analyzed the $NO_3^-$ vs. $PO_4^{3-}$ concentrations across all experiments to estimate the $NO_3^-$:$PO_4^{3-}$ drawdown ratio and its relation to Fe availability in the Amundsen Sea. The initial experimental waters had a $NO_3^-$:$PO_4^{3-}$ drawdown ratio of 21.7 (Fig. 7), which is high relative to Redfield proportions but not unexpected in waters dominated by *P. antarctica* (Arrigo et al., 1999). The unamended control had a $NO_3^-$:$PO_4^{3-}$ utilization ratio approximately equal to 15, with the +Fe and +PA+Fe $NO_3^-$:$PO_4^{3-}$ ratio approximately the same as in the control. The lowest $NO_3^-$:$PO_4^{3-}$ uptake ratio documented were in the +DFB+Fe treatment, which had a significantly lower ratio of 10.8.

In summary, the consistent positive response in $F_v$:$F_m$ but variable responses of Chl *a*, POC, PON, and macronutrient concentrations to the Fe amendments throughout the majority of the sampling region indicate that a photophysiological response to the added Fe took place within the phytoplankton community but that this response was not translated into increased biomass over the course of the experiment. However, the addition of Fe did stimulate the increased consumption of $NO_3^-$ relative to $PO_4^{3-}$ in a majority of experiments, with the open ocean experiment being the lone exception.

## 3.3. Pigment- and group-specific responses to additions

### 3.3.1. Open ocean

Similar to the significant responses detected for Chl *a* and $F_v$:$F_m$ of the open ocean experiment, the concentration of the pigment fucoxanthin in the +Fe and +DFB+Fe treatments was ~1.2-fold greater than that measured in the control (Fig. 8A). In contrast, no increase in the 19′-hex pool was detected when Fe was added alone or complexed to DFB (Fig. 8F). However, both photosynthetic accessory pigments decreased in the +DFB treatment. Despite the lack of significant changes in the 19′-hex concentrations in the +Fe amendments, the Chl *a* normalized 19′-hex ratio did decrease (Fig. 8K), driven primarily by increases in the Chl *a* concentration (Fig. 3A). No changes in the fuco:Chl *a* ratio were observed.

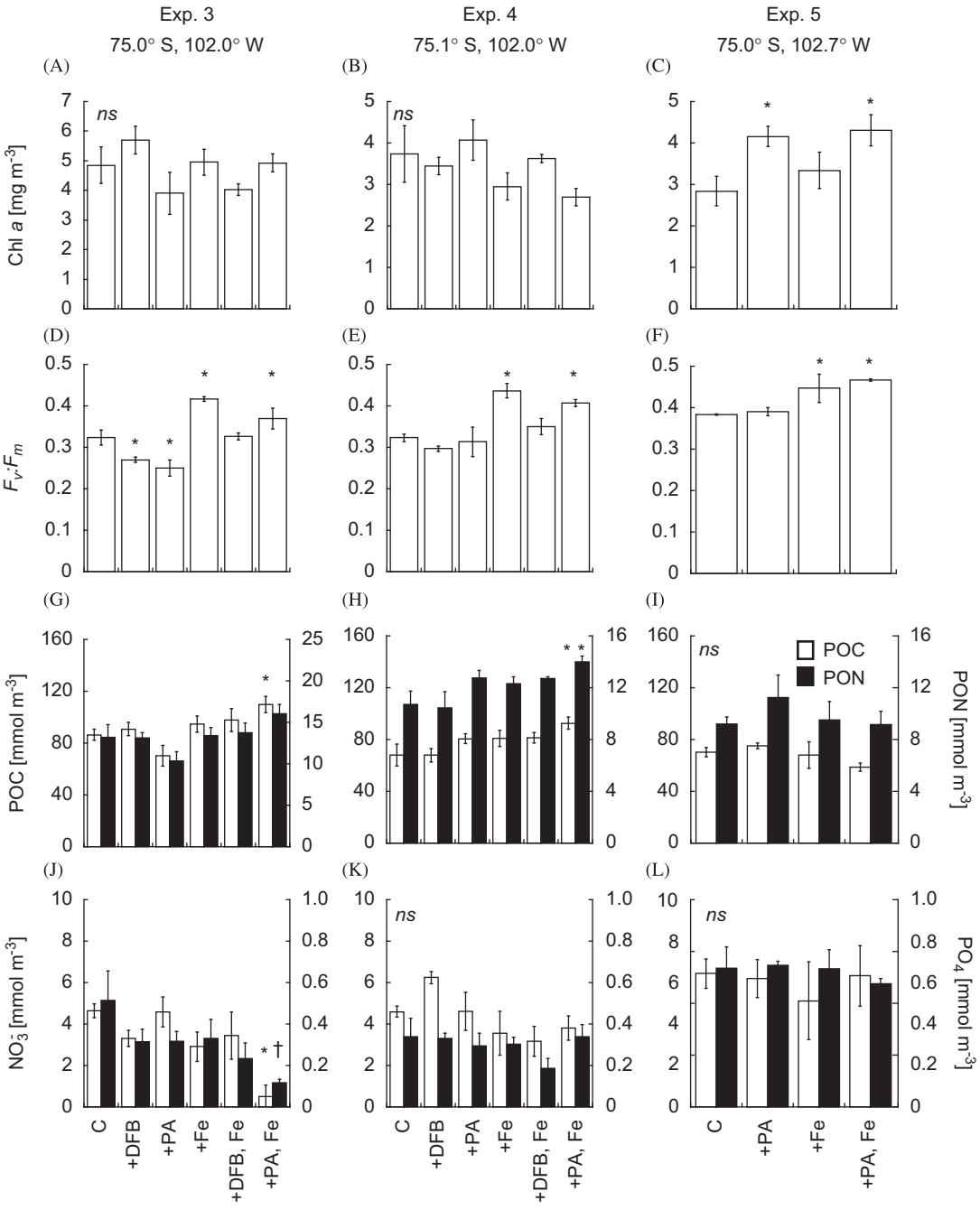


**Fig. 5.** Comparison of (A–C) Chl *a* concentration, (D–F) $F_v$:$F_m$, (G–I) POC and PON concentration, (J-L) and $NO_3^-$ and $PO_4^{3-}$ concentration in the different Fe and ligand treatments from the PIB experiments (Exps. 3, 4, 5). Error bars represent ± 1 standard error. Asterisks (*) indicate significant difference from the control at the $\alpha = 0.05$ significance level. *ns* indicates no significant differences between the control and treatments.

### 3.3.2. MIZ

At the MIZ stations, the changes in the fucoxanthin pool generally mirrored those seen in Chl *a*, with the +Fe response being particularly pronounced in Exps. 2 and 11 (Fig. 8C and E). In contrast, there was a general decrease in the concentration of 19′-hex in all amended treatments (with or without Fe) in Exps. 9 and 11. With the exception of the +DFB and +DFB+Fe treatments, Exp. 1 followed the same trend of fucoxanthin, responding positively to the addition of Fe (Fig. 8B) while 19′-hex decreased (Fig. 8H). The fuco:Chl *a* and 19′-hex:Chl *a* ratios in the MIZ experiments followed a similar trend as that observed in the open ocean experiment, with no between-treatment differences observed in the fuco:Chl *a* ratio, but a decrease in the 19′-hex:Chl *a* ratio in the +Fe treatments. The ligand+Fe treatment generally had a significantly lower 19′-hex:Chl *a* ratio, with the exception of the +DFB+Fe treatments in Exp. 2 and 9. Additionally, the +DFB and +PA only treatments in Exp. 9 had lower 19′-hex:Chl *a* ratios.

### 3.3.3. Polynyas

In experiments conducted within the polynyas, the fuco concentrations remained largely unchanged within all of the amended bottles (Fig. 9A–C). The two exceptions were a reduced fuco concentration, relative to controls, in the +DFB+Fe treatments of Exps. 6 and 8. Changes in fuco in these experiments were similar to changes in bulk Chl *a* (Fig. 4A–C). Decreases in

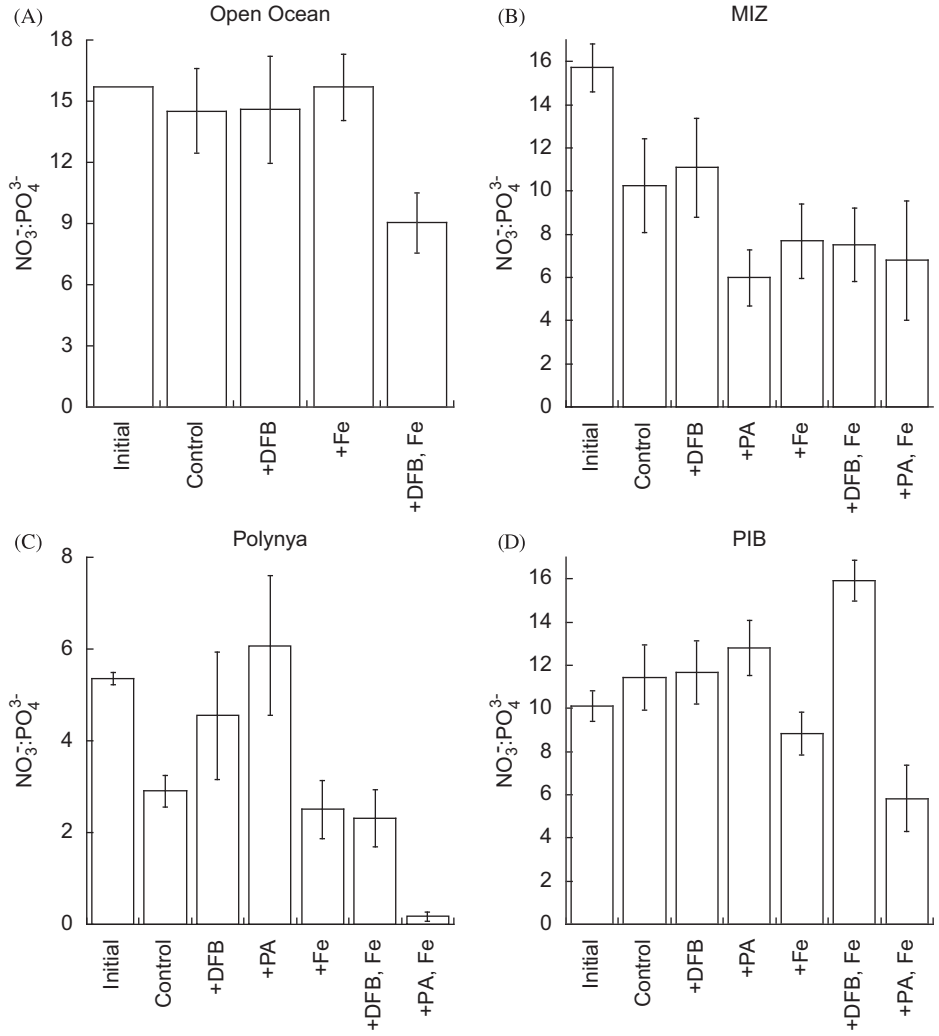


**Fig. 6.** Initial and treatment $NO_3^-:PO_4^{3-}$ ratios averaged across experiments within each experimental type as shown in Fig. 1.

19′-hex relative to the control were observed in almost all treatments with added Fe (Fig. 9D–F). In only the +Fe treatment of Exp. 7 did concentrations of 19′-hex remain unchanged relative to the control. Unlike Exps. 9 and 11 in the MIZ, none of the polynya experiments exhibited changes in 19′-hex when model ligands were added without Fe. When accessory pigments were normalized to Chl *a*, the 19′-hex:Chl *a* ratio declined in all the treatments with added Fe (Fig. 9G–I).

### 3.3.4. Pine Island Bay

Changes in accessory pigments in the experiments conducted at the PIB stations were similar to those in both the MIZ and polynya experiments (Fig. 10). Fuco in the amended treatments was unchanged relative to control concentrations in all three PIB experiments while the concentration of 19′-hex in Exps. 3 and 4 was generally lower than that in the controls (Fig. 10D and E). For example, while the concentration of 19′-hex was unchanged in the +DFB+Fe treatment in Exps. 4, 19′-hex in the +Fe, +PA+Fe treatments were reduced by ~30–70%. In contrast, some treatments amended with only ligands (+DFB in Exp. 3 and +PA in Exp. 5) actually had higher 19′-hex concentrations than the control. When the 19′-hex concentrations were normalized to Chl *a* concentrations, the effect of the added Fe was even more pronounced, with all treatments amended with Fe having significantly lower concentrations of 19′-hex than the control across all experiments at PIB stations (Fig. 10G and H).

### 3.4. Availability of organically bound Fe

The availability of Fe bound to the model ligands was assessed by regressing the Chl *a*, $F_v$:$F_m$, POC, PON, and the accessory pigments (fuco and 19′-hex) responses in the ligand+Fe treatments against their responses in the +Fe treatments across all experiments (Fig. 11A–D). A slope greater (less) than 1.0 suggests greater (less) Fe availability in the ligand+Fe treatment. In general, adding Fe bound to the model ligands did not result in greater responses relative to Fe added alone, and in several cases, the responses decreased. For example, pigment concentrations in treatments with Fe complexed to both DFB and PA were ~5–40% lower relative to free Fe (Fig. 11A–C), with one exception. Fuco concentrations in the +PA+Fe treatment were not statistically different from that measured in the +Fe treatments. Despite the lower pigment concentrations in the ligand+Fe treatments relative to the free Fe treatment, $F_v$:$F_m$ was the same independent of whether Fe was complexed or not (Fig. 11D). Likewise, both POC and PON were not significantly different between the different Fe treatments (data not shown). Thus, while the difference between the ligand+Fe and the +Fe treatments may suggest that Fe bound to the model ligands was less bioavailable, the lack of a

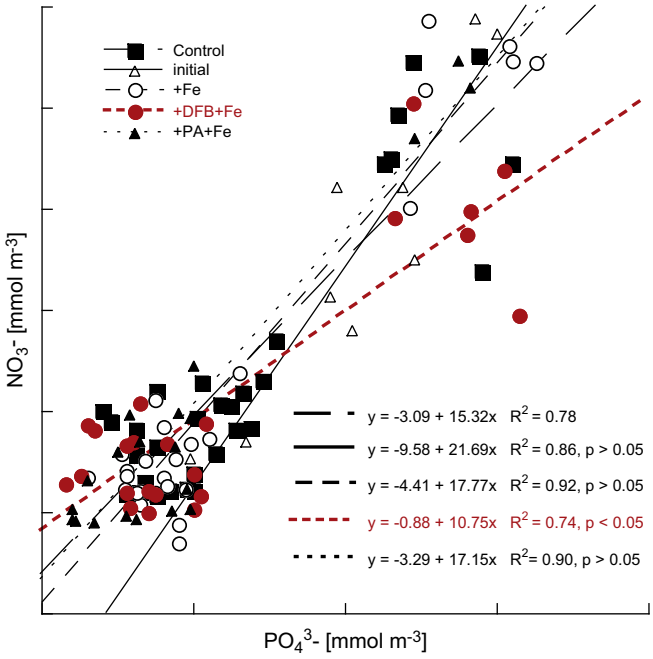


**Fig. 7.** $NO_3^-$ vs. $PO_4^{3-}$ concentrations in the initial, control, +Fe, and +ligand+Fe treatments of the bioassay experiments. Shown are the least squared linear fits, the resulting adjusted $R^2$ values for each treatment, and p values indicating difference from control at the $\alpha=0.05$ significance level.

difference in $F_v$:$F_m$ between these treatments suggests any bioavailabilty differences did not translate to biomass differences.

## 4. Discussion

### 4.1. Phytoplankton response to added Fe

At the time of our investigation, there were intense phytoplankton blooms in both the AP and the PIP, with Chl *a* and POC concentrations reaching as high as 13 mg Chl *a* $m^{-3}$ and 87 mmol C $m^{-3}$, respectively (Alderkamp et al., 2012). The phytoplankton community in both blooms was composed primarily of *P. antarctica* ( > 60% of the phytoplankton community). These two polynyas consistently have the highest Chl *a* concentrations of all the Antarctic polynyas (Arrigo and van Dijken, 2003), although the blooms during our investigation were modest by comparison to other years (Arrigo et al., 2012).

DFe concentrations within the bloom were at levels previously shown to limit phytoplankton growth in the Southern Ocean (see review by Boyd et al. (2007)). In our experiments, additions of bioavailable Fe consistently resulted in increased $F_v$:$F_m$, decreased concentrations of the accessory pigment 19′-hex (as well as lower 19′-hex:Chl *a* ratios), and an increase in the utilization of $NO_3^-$ relative to $PO_4^{3-}$.

Increased $F_v$:$F_m$ over very short time scales ( < 2 day) has been demonstrated in both mesoscale Fe addition experiments and in investigations of natural Fe fertilization in the Southern Ocean and has been used as an indicator of relief from Fe-limitation (Kolber et al., 1994, Behrenfeld et al., 1996; Coale et al., 1996; Boyd et al., 1998, 2000; Boyd and Abraham 2001; Boyd, 2002, Moore et al., 2006; Berg et al., 2011). The likely mechanism for this increase in $F_v$:$F_m$ is an Fe-induced increase in the number of functional reaction centers, either through repair of damaged reaction centers or through de novo synthesis of new ones (Greene et al., 1991). However, changes in $F_v$:$F_m$ due to shifts in the taxonomic composition can swamp signals due to physiological changes, although this is believed to be less prevalent in HNLC environments (Suggett et al., 2009). In some of our experiments, Fe-induced increases in $F_v$:$F_m$ did correspond to increases in fuco concentrations, which we interpret as indicative of an increase in the diatom fraction of the Chl *a* pool. However, this was observed only in the offshore experiment (Exp. 12) and in two MIZ experiments (Exp. 2 and 11). In most of our Fe addition experiments, increases in $F_v$:$F_m$ were not associated with shifts in the diatom fraction of the Chl *a* pool. As such, we interpret the increases in $F_v$:$F_m$ as relief from Fe stress induced by low Fe availability.

The decline in the 19′-hex:Chl *a* ratios we observed in the Fe-amended treatments is consistent with our conclusion that *P. antarctica* populations in-situ were experiencing Fe stress. A decrease in absolute concentrations of 19′-hex, rather than an increase in Chl *a* concentrations, were the likely cause of this decreased ratio. Decreased cellular concentrations of 19′-hex have been noted in N-limited and P-limited cultures of the haptophyte *Emiliana huxleyi* and have been hypothesized to be a consequence of low growth rates that result in lowered dilution rates of 19′-hex in daughter cells relative to the production of 19′-hex (Stolte et al., 2000). If this hypothesized mechanism holds in Fe stressed *P. antarctica* as well, then relief from Fe stress may increase growth rates and thus 19′-hex dilution rates in daughter cells. Previous investigations have demonstrated that the ratio of 19′-hex:Chl *a* in *P. antarctica* cultures increases during Fe-limitation, with values exceeding 1.0 (van Leeuwe and Stefels, 1998; DiTullio et al., 2007; Alderkamp et al., 2012). Although the initial 19′-hex:Chl *a* ratios in our experiments were all < 1 (with the exception of Exp. 6), the consistent decreases in the 19′-hex:Chl *a* ratio we observed after addition of Fe indicated that *P. antarctica* had been experiencing some Fe stress prior to the start of our experiments. However, the low initial 19′-hex:Chl *a* ratio and the presence of blooming populations of *P. antarctica* during our study indicate that *P. antarctica* was not chronically Fe-limited over most of the Amundsen Sea, and perhaps had acclimated to low Fe concentrations (Alderkamp et al., 2012). The relatively high initial $F_v$:$F_m$ values ( ≥ 0.4) at most stations is consistent with a lack of chronic Fe limitation.

### 4.2. Availability of organically bound Fe

The phytoplankton blooms in the PIP and the AP during the 2008–2009 season lasted ~70 days (Arrigo et al., 2012) and the experiments described here were conducted between days 38 and 66. During much of this period, rates of primary productivity in the PIP either increased or remained above 1 g C $m^{-2}$ $d^{-1}$ while rates in the AP dropped, but were generally > 0.4 g C $m^{-2}$ $d^{-1}$ (Arrigo et al., 2012). The concentrations of DFe in the polynyas at this time were potentially limiting (ranging from 0.09–0.25 nmol $L^{-1}$ in the bioassay experiments), and our bioassay experiments indicate that the phytoplankton communities were under some level of Fe stress. The relatively high productivity, yet potentially limiting concentrations of DFe, raises questions about the identity of the Fe sources that supported the AP and PIP phytoplankton blooms.

The primary sources of Fe in this region are believed to be upwelling at the ice shelf face, lateral turbulent diffusion, and sea ice melt (Gerringa et al., 2012). The upwelling Fe source is a combination of warm MCDW that travels along the bottom of the continental shelf to the ice shelf cavity, where its higher temperature melts the ice shelf from below, and glacial Fe is subsequently released into the MCDW. This glacial ice melt modifies the MCDW and results in a buoyant plume of meltwater MCDW rich in both macronutrients and Fe that upwells from below the ice shelf at a few locations in front of the PIG. A Fe budget estimated for the Amundsen Sea suggests that concentrations of DFe in the upwelled meltwater MCDW are high enough to support measured rates of phytoplankton productivity, assuming

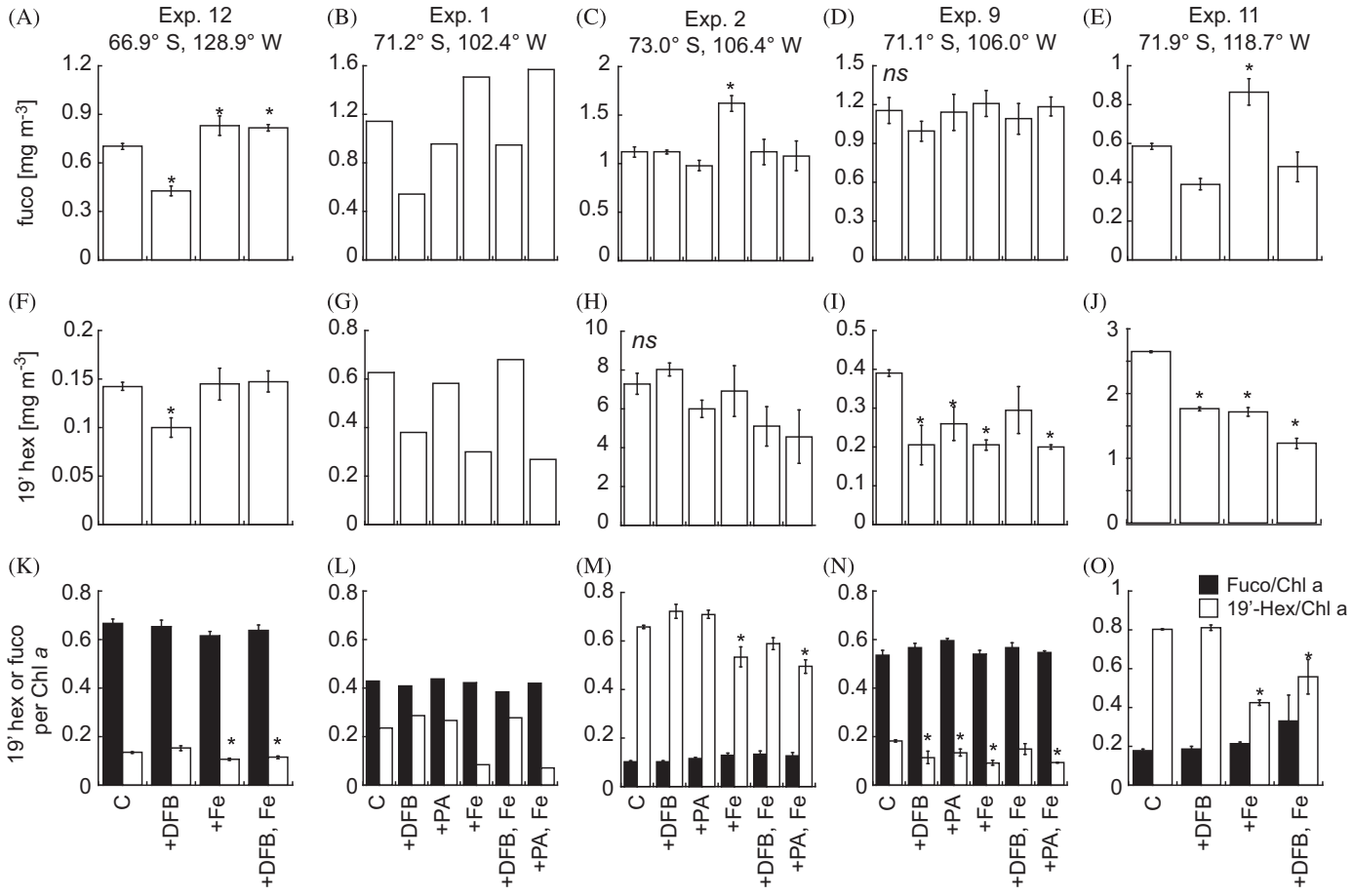


**Fig. 8.** Comparison of (A–E) fucoxanthin (fuco) concentration, (F–J) 19′-hexanoylfucoxanthin (19′-hex) concentration, and (K–O) the 19′-hex:Chl *a* or fuco:Chl *a* ratio in the different Fe and ligand treatments from the open ocean (Exp. 12) and the MIZ (Exps. 1, 2, 9, 11) experiments. Error bars represent ± 1 standard error. Asterisks (∗) indicate significant difference from the control at the $\alpha=0.05$ significance level. *ns* indicates no significant differences between the control and treatments.

that they are advected laterally into the adjacent polynyas and are bioavailable (Gerringa et al., 2012).

Results from our bioassays suggest that while Fe bound to the model ligands PA and DFB was less available to the phytoplankton, some of the complexed Fe was still available. However, the degree of bioavailability varies for each of the Fe–ligand complexes. Fe bound to PA was likely the more available form of organically complexed Fe, while Fe bound to DFB was less available. This is evidenced by the positive $F_v$:$F_m$ responses relative to the controls in seven of eight experiments with +PA+Fe treatments while only 4 of 10 experiments that had +DFB+Fe treatments exhibited positive responses (Figs. 3–5). Comparatively, eight of eleven +Fe treatments showed enhanced $F_v$:$F_m$ relative to the controls. Likewise, the fuco concentrations were similar between +Fe and +PA+Fe treatments, but were reduced in the +DFB+Fe amended bottles (Fig. 10B). DFB is a hexatentate hydroxamate fungal siderophore (Keller-Schierlein et al., 1965, Mueller and Raymond, 1984) that binds the Fe molecule at six sites, the likely reason for its low bioavailability. PA is only a tridentate P-containing organic ligand (Graf et al., 1987), potentially making it more bioavailable. The relative degree of bioavailability observed for the different ligand+Fe complexes observed in this study agrees well with previous observations. Fe bound to PA has been shown to be readily available to phytoplankton (Maldonado et al., 2005, Hassler and Schoemann, 2009) while Fe complexed to DFB has been demonstrated to be less available (Wells, 1999; Wells and Trick, 2004). Though availability of DFB-bound Fe increases over time likely the result of thermal, chemical, or biological decomposition of DFB (Kuma et al., 2000). Likewise, Hutchins et al. (1999) showed that uptake of Fe was lowest when bound to hydroxamates (ferrioxamine and ferrichrome) while Eldridge et al. (2004) demonstrated a decrease in picoeukaryote cell size with decreasing Fe availability due to enhanced complexation with the ligand DFB.

Despite the ligand dependent differences in Fe bioavailability indicated by the changes in $F_v$:$F_m$ and pigment concentrations, there was little difference in Fe bioavailability indicated by the biomass and nutrient variables. In fact, POC, PON, $NO_3^-$, and $PO_4^{3-}$ concentrations did not differ between the Fe amended treatments. The likely reason for this is that any changes in pigment concentration (e.g. decrease in accessory pigments in the +Fe treatments) were likely compensated for by the increased $F_v$:$F_m$ in these same treatments. Previous work has shown that addition of Fe to Southern Ocean waters increases maximum photosynthetic quantum yield without corresponding increases in the maximum biomass-specific productivity rate (Hiscock et al., 2008). Thus, when Fe was depleted or unavailable, the phytoplankton likely maintained their productivity at reduced efficiency with higher concentrations of accessory pigments. However, when Fe was made available, cells likely increased their photosynthetic efficiency and decreased the concentration of accessory pigments (primarily 19′-Hex).

During our investigation, the concentration of organic ligands decreased along a gradient northwestward from the ice shelves into the polynyas, indicating that the meltwater MCDW upwelling from below the ice shelf was a major source of ligands to the

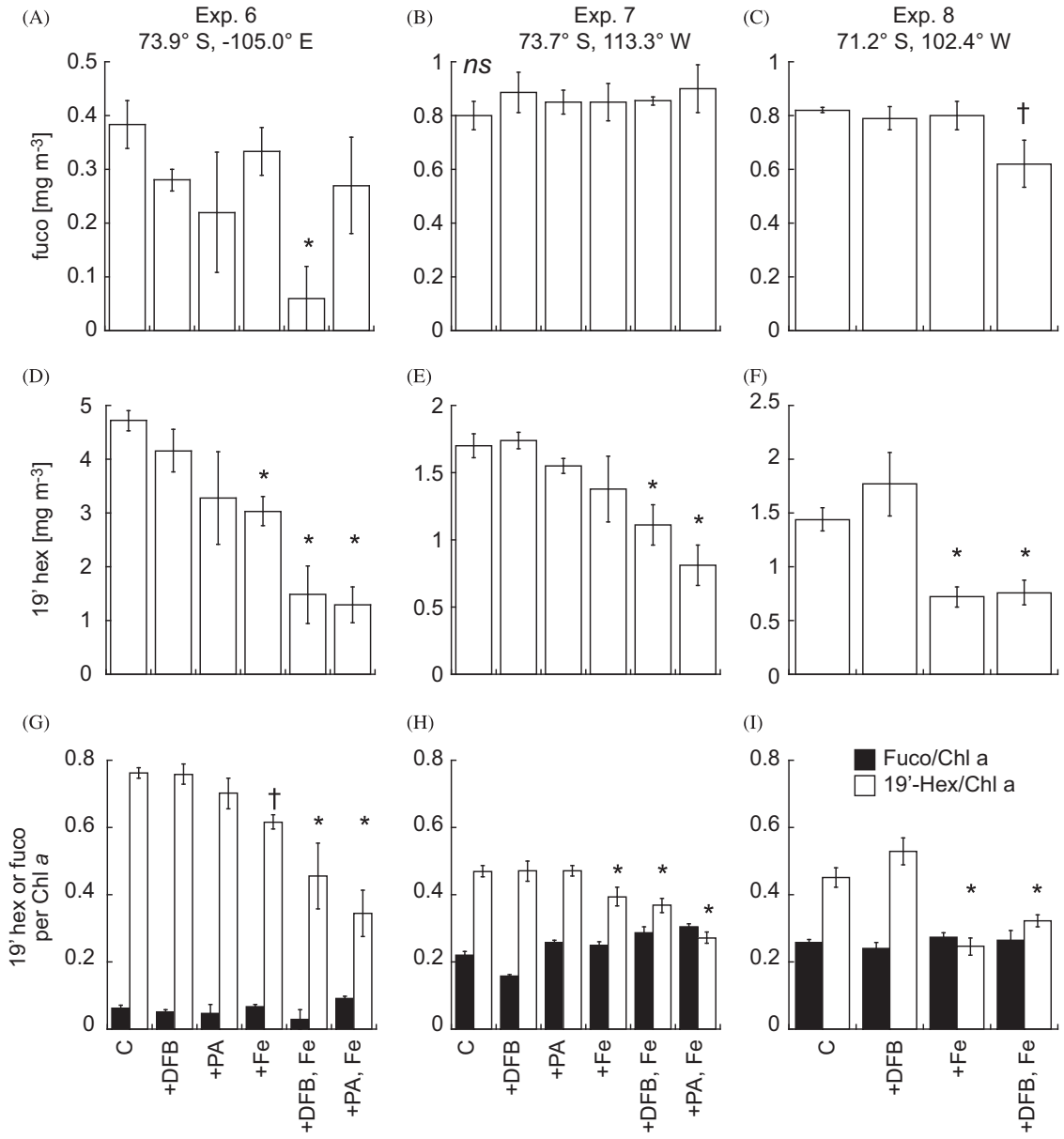


**Fig. 9.** Comparison of (A–C) fuco concentration, (D–E) 19′-hex concentration, and (G–I) the 19′-hex:Chl *a* or fuco:Chl *a* ratio, in the different treatments from the polynya experiments (Exps. 6, 7, 8). Error bars represent ± 1 standard error. Asterisks (*) and crosses (†) indicate significant difference from the control at the $\alpha$=0.05 and 0.07 significance levels, respectively. *ns* indicates no significant differences between the control and treatments.

region (Thuróczy et al., 2012). In contrast to ligand concentration, the saturation of the ligand pool decreased along this gradient, with more excess ligand in the center of the AP and the PIP, and thus a greater capacity for the ligand pool to enhance Fe availability. The measured stability constants ($\log K'$) of the natural ligand pool ranged from 21.28 to 22.96 $mol^{-1}$ and were similar to those of the model ligands used in our experiments ($\log K'_{DFB}$=21.8 $mol^{-1}$, $\log K'_{PA}$= 20.8 $mol^{-1}$, Maldonado et al., 2005). While the similarity of the conditional stability constants is one indicator that the availability of the model ligands used here may be analogous to the availability of the in-situ natural ligand pool, other factors, such as the ability of cellular Fe uptake systems to recognize and reduce organic complexes, plays a major role in determining the bioavailability of ligand-bound Fe.

In addition to the upwelled meltwater MCDW ligand source, the blooming phytoplankton may be an important ligand source. Recent evidence shows that saccharides and uronic acids produced by phytoplankton under a variety of environmental conditions act as weak binding ligands that form highly bioavailable colloidal Fe complexes (Hassler et al., 2011). In fact, the colony matrix of *P. antarctica*, which dominated the phytoplankton blooms during our study, is composed of mucopolysaccharides (Alderkamp et al., 2007). Culture experiments showed that the uptake of Fe by *P. antarctica* was enhanced ~2 fold in incubations where the polysaccharide dextran was added (Hassler et al., 2011). It seems that organic complexation of Fe in the Amundsen Sea enhances the availability of Fe to phytoplankton and contributes to the persistent blooms in both the AP and the PIP (Thuróczy et al., 2012).

### 4.3. Fe and $NO_3^-$ interactions

The primary use of Fe in phytoplankton physiology is as a cofactor in photosynthetic light harvesting and electron transport proteins, as well as in N metabolism enzymes (e.g. nitrate and nitrite reductase). As such, both photosynthesis and N utilization

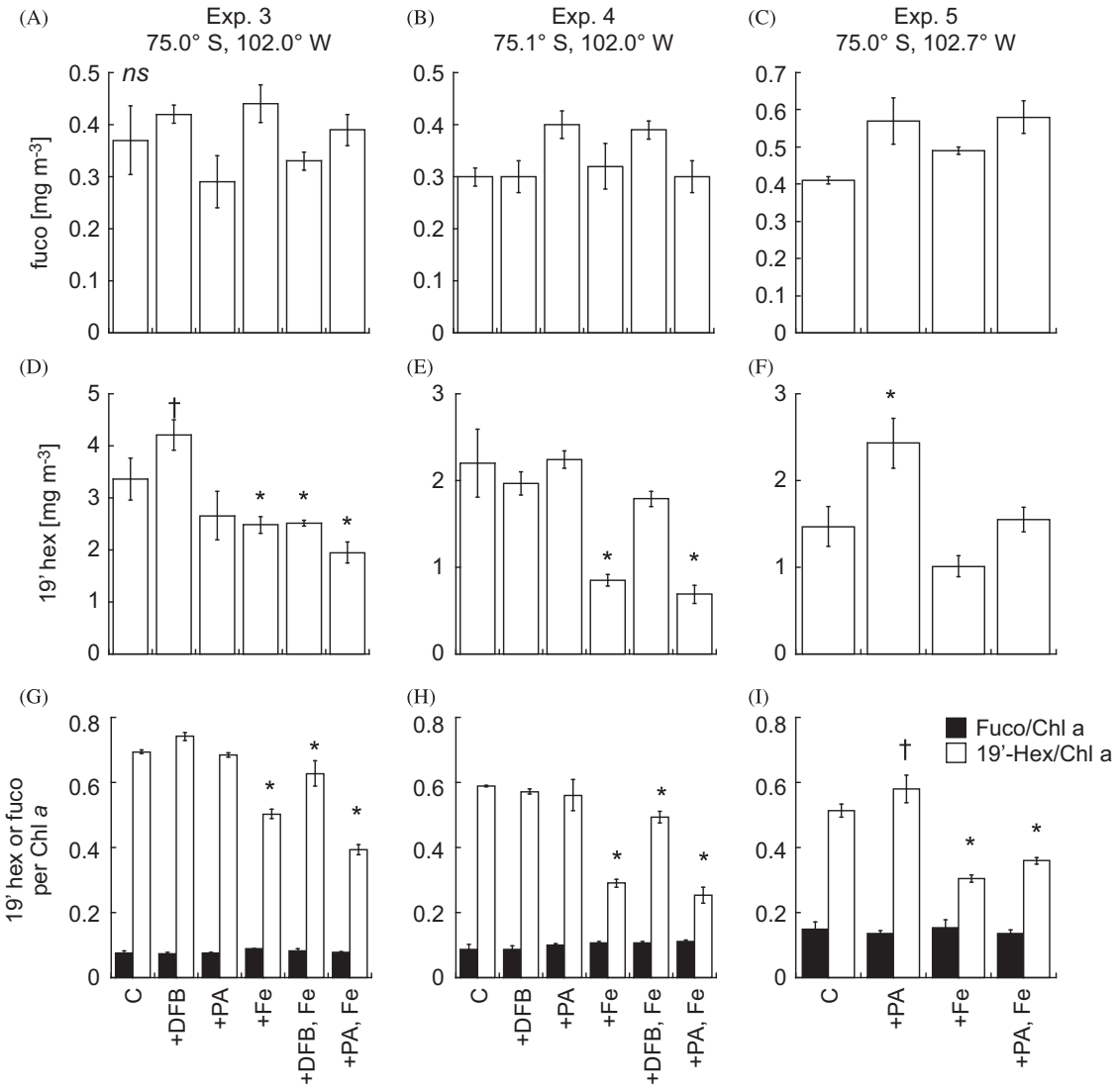


**Fig. 10.** Comparison of (A–C) fuco concentration, (D–E) 19′-hex concentration, and (G–I) the 19′-hex:Chl *a* or fuco:Chl *a* ratio in the different Fe and ligand treatments from the PIB experiments (Exps. 3, 4, 5). Error bars represent ± 1 standard error. Asterisks (*) and crosses (†) indicate significant difference from the control at the $\alpha = 0.05$ and 0.07 significance levels respectively. *ns* indicates no significant differences between the control and treatments.

are affected at reduced Fe concentrations such as those encountered in the Amundsen Sea.

Sea surface temperatures and salinities indicate that ice melt contributed to the shallow mixed layers (~19 m) in the PIP (Fig. 3; Alderkamp et al., 2012). Ice melt is a source of Fe to polynya waters (Gerringa et al., 2012; Van Der Merwe et al., 2009) and has been suggested to drive the near-complete consumption of mixed layer $NO_3^-$ by phytoplankton (Moline and Prezelin, 1997). Consistent with this, more $NO_3^-$ was taken up relative to $PO_4^{3-}$, as indicated by the change in the $NO_3^-$:$PO_4^{3-}$ ratio of the initial vs. Fe treated waters. Likewise, across the MIZ, PIP, and PIB sites, the majority of the Fe amended treatments had a mean $NO_3$:$PO_4$ ratio that was lower than in the controls, suggesting that $NO_3^-$ uptake was stimulated in the +Fe bottles. Significantly lower $NO_3^-$ concentrations in Fe amended bottles relative to controls treatments were also observed in several of our experiments. The Fe stimulated uptake of $NO_3^-$ highlights the requirement of Fe for $NO_3^-$ reduction in phytoplankton.

Little is known about how Fe is allocated within cells when Fe availability is low, although there is plenty of evidence to show that proteins within the photosynthetic machinery are the greatest cellular sinks of Fe in phytoplankton (Veldhuis et al., 2005; Strzepek and Harrison, 2004). Fe is a vital component in the reaction center proteins of PS I and II, as well as in the cytochrome $b_6$/f complex (Falkowski and Raven, 1997). Equally well documented though is the increased utilization of $NO_3^-$ upon relief from Fe-limitation in phytoplankton (Berg et al., 2011; Hutchins et al., 2002). The $NO_3^-$ and $NO_2^-$ reducing enzymes, nitrate and nitrite reductase, both contain Fe as a trace metal cofactor in their active site and their activity is proportional to the availability of Fe (Milligan and Harrison, 2000).

Consistent with this finding is the pattern of the $NO_3^-$:$PO_4^{3-}$ drawdown ratio when data from all 11 bioassays are combined (Fig. 7). Here, $NO_3^-$:$PO_4^{3-}$ uptake ratios were lowest when Fe was provided in its most unavailable form (DFB-bound). In contrast, uptake ratios in the +Fe, and +PA+Fe, and were approximately equal to the unamended control. These data support the finding that greater Fe availability is associated with increased drawdown of $NO_3^-$ relative to $PO_4^{3-}$, and suggest that the in-situ community had access to available Fe. Enhanced $NO_3^-$:$PO_4^{3-}$ drawdown ratios at elevated Fe concentrations have been documented in multiple studies (Moore et al., 2007; Price, 2005; Hutchins et al., 2002; De Baar et al., 1997) and have been explained either as enhanced $NO_3^-$ uptake and reduction at high Fe concentrations

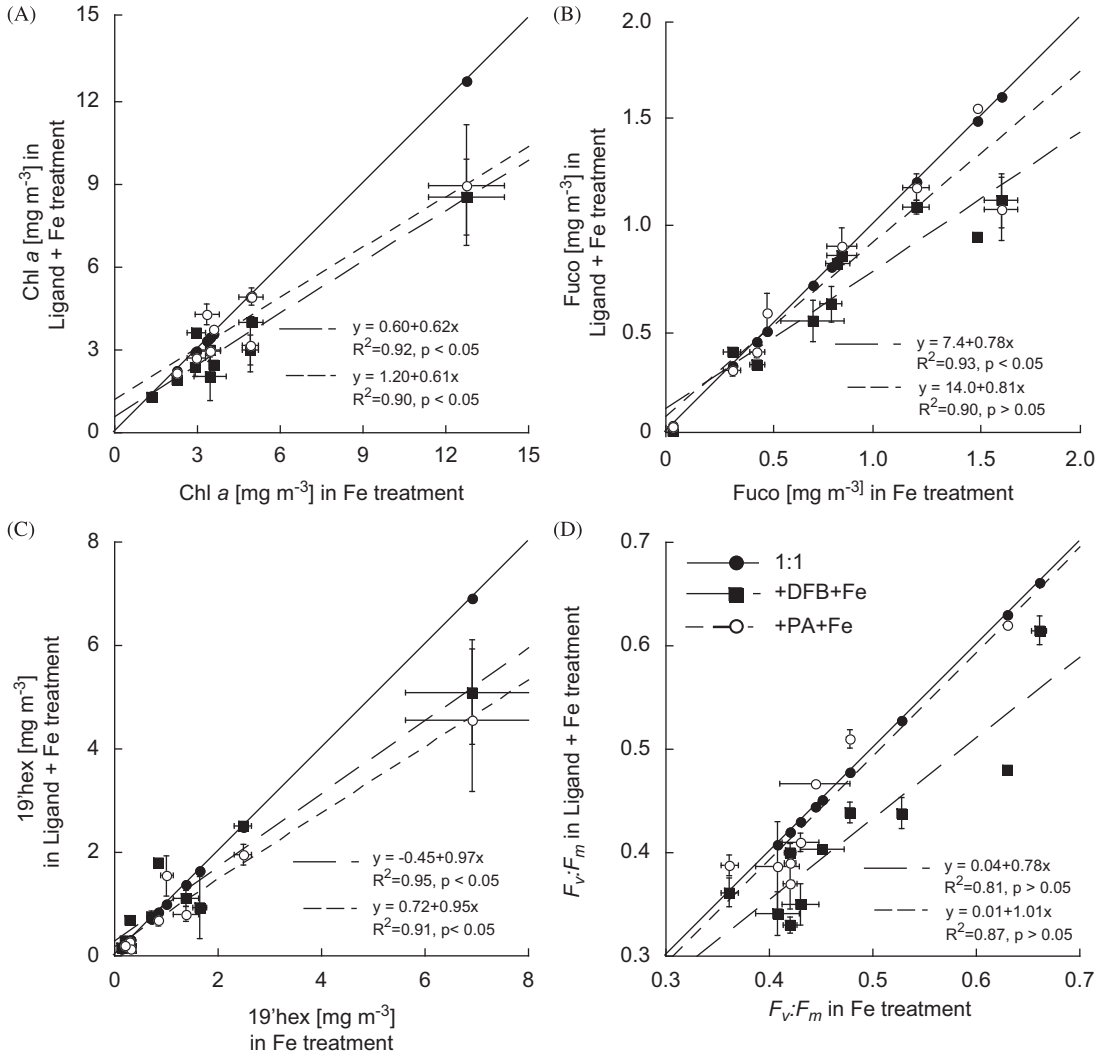


**Fig. 11.** Response of (A) Chl *a*, (B) fucoxanthin (C) 19′-hexanoylfucoxanthin concentrations, and (D) $F_v$:$F_m$, in the +Fe alone vs. the +ligand+Fe treatments. The solid line represents the 1:1 +Fe response. Shown are the least squared linear fits, the resulting adjusted $R^2$ values for each treatment, and p values indicating difference from control at the $\alpha$=0.05 significance level.

(De Baar et al., 1997), decreased per cell concentrations of P under high Fe availability (Price, 2005), or shifts to phytoplankton taxa with higher $NO_3^-$:$PO_4^{3-}$ drawdown ratios. The lowered $NO_3$:$PO_4$ ratio in the +Fe and +PA+Fe treatments suggests that $NO_3^-$ consumption increased. Combined with the lack of a major shift in the phytoplankton community, as indicated by the constant fuco concentrations, we suggest that this Fe-dependent increase in the $NO_3^-$:$PO_4^{3-}$ utilization ratio is consistent with a greater uptake of $NO_3^-$.

In the Ross Sea, the $NO_3^-$:$PO_4^{3-}$ utilization ratios differ markedly between phytoplankton taxa, with diatoms having a low (~9) and *P. antarctica* having a high (~19) utilization ratio (Arrigo et al., 1999). Taxonomic differences in N species utilization may drive some of this difference; with diatoms relying on mixed species of N (i.e. $NO_3^-$ and $NH_4^+$) for growth while *P. antarctica* relies more heavily on $NO_3^-$. Here we show that Fe plays a vital role in $NO_3^-$:$PO_4^{3-}$ drawdown, especially in *P. antarctica* dominated waters, by providing a vital element necessary for $NO_3^-$ reduction. As such, the relatively high $NO_3^-$:$PO_4^{3-}$ utilization ratios observed in the *P. antarctica* dominated portions of the Ross Sea indicate a relatively high degree of Fe bioavailability. Thus the $NO_3^-$:$PO_4^{3-}$ uptake ratio may be a diagnostic tool for Fe-limitation.

In summary, the proximity of the Amundsen Sea to upwelling meltwater MCDW and glacial melt waters make it an area of relatively high total Fe input compared with other Antarctic environments (Gerringa et al., 2012; Thuróczy et al., 2012). The vast majority of this Fe is bound to organic matter and may not be not freely available for direct uptake by phytoplankton. Despite this, some of the largest blooms in coastal Antarctic waters are found in the Amundsen Sea (Arrigo and van Dijken, 2003). Our work shows that the phytoplankton bloom that formed during the austral summer of 2009 was likely able to use much of this organically bound Fe. Additionally, we suggest that the Fe taken up during our experiments resulted in the increased uptake of $NO_3^-$. As a consequence, the bioavailability of Fe directly affects the $NO_3^-$:$PO_4^{3-}$ utilization ratio, with higher ratios associated with more bioavailable Fe.

The dominant phytoplankton taxa throughout much of the Amundsen and the Ross Seas is *P. antarctica* (Alderkamp et al., 2012; Arrigo et al., 1999), which produces and releases saccharides, organic compounds known to act as ligands that increase the bioavailability of Fe (Hassler et al., 2011). Thus, the previously observed correlation between *P. antarctica* and high $NO_3^-$:$PO_4^{3-}$ utilization ratios (Arrigo et al., 1999) may be a result of *P. antarctica's* ability to increase the bioavailability of Fe enhancing its ability to take up $NO_3^-$.

## Acknowledgments

The authors would like to acknowledge the Captain and crew of R.V. *Nathaniel B. Palmer*, as well as, Stanley Jacobs, the chief scientist during the NBP09-01 cruise. Funding for this Project was provided by a National Science Foundation grant to KRA (ANT-0732535) as part of the International Polar Year, and by the Netherlands Organization for Scientific Research (NWO), Netherlands AntArctic Program (NAAP grant 851.20.041).

## References

Alderkamp, A.C., Mills, M.M., van Dijken, G.L., Laan, P., Thuroczy, C.E., Gerringa, L., de Baar, H.J.W., Payne, C., Tortell, P., Visser, R.J.W., Buma, A.G.J., Arrigo, K.R., 2012. Iron from melting glaciers fuels phytoplankton blooms in Amundsen Sea (Southern Ocean); phytoplankton characteristics and productivity. Deep-Sea Res. II 71–76, 32–48.

Alderkamp, A.C., Kulk, G., Buma, A.G.J., Van Dijken, G.L., Mills, M.M., Visser, R.W., Arrigo, K.R., 2012. The effect of iron limitation on the photophysiology of *Phaeocystis antarctica* and *Fragilariopsis cylindrus* under dynamic irradiance. J. Phycol. 48, 45–59.

Alderkamp, A.C., Buma, A.G.J., van Rijssel, M., 2007. The carbohydrates of *Phaeocystis* and their degradation in the microbial food web. Biogeochemistry 83 (1-3), 99–118.

Arrigo, K.R., Lowry, K.E., van Dijken, G.L., 2012. Annual changes in sea ice and phytoplankton in polynyas of the Amundsen Sea, Antarctica. Deep-Sea Res. II 71–76, 5–15.

Arrigo, K.R., van Dijken, G.L., 2003. Phytoplankton dynamics within 37 Antarctic coastal polynya systems. J. Geophys. Res.—Oceans 108 (C8).

Arrigo, K.R., Robinson, D.H., Worthen, D.L., Dunbar, R.B., DiTullio, G.R., VanWoert, M., Lizotte, M., 1999. Phytoplankton community structure and the drawdown of nutrients and $CO_2$ in the Southern Ocean. Science 283, 365–367.

Arrigo, K.R., Worthen, D.L., Schnell, A., Lizotte, M.P., 1998. Primary production in Southern Ocean waters. J. Geophys. Res. 103, 15587–15600.

Behrenfeld, M.J., Bale, A.J., Kolber, Z.S., Aiken, J., Falkowski, P.G., 1996. Confirmation of iron limitation of phytoplankton photosynthesis in the equatorial Pacific Ocean. Nature 383 (6600), 508–511.

Benner, R., 2011. Loose ligands and available iron in the ocean. Proc. Natl. Acad. Sci. USA 108 (3), 893–894.

Berg, G.M., Mills, M.M., Long, M.C., Bellerby, R., Strass, V., Savoye, N., Rottgers, R.R., Croot, P.L., Webb, A., Arrigo, K.R., 2011. Variation in particulate C and N isotope composition following iron fertilization in two successive phytoplankton communities in the Southern Ocean. Global Biogeochem. Cycles 25, GB3013. http://dx.doi.org/10.1029/2010GB003824.

Boyd, P., Berges, J.A., Harrison, P.J., 1998. In vitro iron enrichment experiments at iron-rich and -poor sites in the NE subarctic Pacific. J. Exp. Mar. Biol. Ecol. 227 (1), 133–151.

Boyd, P., Watson, A., Law, C., Abraham, E., Trull, T., Murdoch, R., Bakker, D., Bowie, A., Buesseler, K., Chang, H., Charette, M., Croot, P., Downing, K., Frew, R., Gall, M., Hadfield, M., Hall, J., Harvey, M., Jameson, G., LaRoche, J., Liddicoat, M., Ling, R., Maldonado, M., McKay, R., Nodder, S., Pickmere, S., Pridmore, R., Rintoul, S., Safi, K., Sutton, P., Strzepek, R., Tanneberger, K., Turner, S., Waite, A., Zeldis, J., 2000. A mesoscale phytoplankton bloom in the polar Southern Ocean stimulated by iron fertilization. Nature 407 (6805), 695–702.

Boyd, P.W., 2002. The role of iron in the biogeochemistry of the Southern Ocean and equatorial Pacific: a comparison of in situ iron enrichments. Deep-Sea Res. II 49 (9-10), 1803–1821.

Boyd, P.W., Abraham, E.R., 2001. Iron-mediated changes in phytoplankton photosynthetic competence during SOIREE. Deep-Sea Res. II 48 (11–12), 2529–2550.

Boyd, P.W., Jickells, T., Law, C.S., Blain, S., Boyle, E.A., Buesseler, K.O., Coale, K.H., Cullen, J.J., de Baar, H.J.W., Follows, M., Harvey, M., Lancelot, C., Lavasseur, M., Owens, N.P.J., Pollard, R., Rivkin, R.B., Sarmiento, J., Schoemann, V., Smetacek, W., Takeda, S., Tsuda, A., Turner, S., Watson, A.J., 2007. Mesoscale iron enrichment experiments 1993-2005: Synthesis and future directions. Science 315, 612–617.

Boyd, P.W., Ellwood, M.J., 2010. The biogeochemical cycle of iron in the global ocean. Nat. Geosci. 3, 675–682.

Coale, K.H., et al., 1996. A massive phytoplankton bloom induced by an ecosystem-scale iron fertilization experiment in the equatorial Pacific Ocean. Nature 383, 495–501.

Croot, P.L., Johanson, M., 2000. Determination of iron speciation by cathodic stripping voltammetry in seawater using the competing ligand 2-(2-Thiazolylazo)-p-cresol (TAC). Electroanalysis 12, 565–576.

De Baar, H.J.W., Boyd, P.W., Coale, K.H., Landry, M.R., Tsuda, A., Assmy, P., Bakker, D.C.E., Bozec, Y., Barber, R.T., Brzezinski, M.A., Buesseler, K.O., Boye, M., Croot, P.L., Gervais, F., Gorbunov, M.Y., Harrison, P.J., Hiscock, W.T., Laan, P., Lancelot, C., Law, C.S., Levasseur, M., Marchetti, A., Millero, F.J., Nishioka, J., Nojiri, Y., van Oijen, T., Riebesell, U., Rijkenberg, M.J.A., Saito, H., Takeda, S., Timmermans, K.R., Veldhuis, M.J.W., Waite, A.M., Wong, C.S., 2005. Synthesis of iron fertilization experiments: from the iron age in the age of enlightenment. J. Geophys. Res.—Oceans 110 (C9).

De Baar, H.J.W., van Leeuwe, M.A., Scharek, R.A., Goeyens, L., Bakker, K., Fritsche, P., 1997. Nutrient anomalies in *Fragilariopsis kerguelensis* blooms, iron deficiency and the nitrate/phosphate ratio (A.C. Redfield) of the Antarctic Ocean. Deep-Sea Res. II 44 (1/2), 229–260.

De Baar, H.J.W., Gerringa, L.J.A., Laan, P., Timmermans, K.R., 2008. Efficiency of carbon removal per added iron in ocean iron fertilization. Mar. Ecol. —Prog Ser. 364, 269–282.

De Jong, J.T.M., den Das, J., Bathmann, U., Stoll, M.H.C., Kattner, G., Nolting, R.F., De Baar, H.J.W., 1998. Dissolved iron at subnanomolar levels in the Southern Ocean as determined by ship-board analysis. Anal. Chim. Acta 377 (2-3), 113–124.

DiTullio, G.R., Garcia, N.S., Rieseman, S.F., Sedwick, P.N., 2007. Effects of iron concentrations in Phaeocystis antarctica grwon at low irradiance. Biogeochemistry 83, 71–81.

Eldridge, M.L., Trick, C.G., Alm, M.B., DiTullio, G.R., Rue, E.L., Bruland, K.W., Hutchins, D.A., Wilhelm, S.W., 2004. Phytoplankton community response to a manipulation of bioavailable iron in HNLC waters of the subtropical Pacific Ocean. Aqua. Microb. Ecol. 35, 79–91.

Falkowski, P.G., 1997. Evolution of the nitrogen cycle and its influence on the biological sequestration of $CO_2$ in the ocean. Nature 387, 272–275.

Falkowski, P.G., Raven, J.A., 1997. Aquatic Photosynthesis. Blackwell Science, Malden, MA, USA.

Gerringa, L.J.A., Alderkamp, A.C., Laan, P., Thuróczy, C.E., de Baar, H.J.W., Mills, M.M., van Dijken, G.L., van Haren, H., Arrigo, K.R., 2012. Iron from melting glaciers fuels the phytoplankton blooms in Amundsen Sea (Southern Ocean): Iron biogeochemistry. Deep-Sea Res. II 71–76, 16–31.

Graf, E., Empson, K.L., Eaton, J.W., 1987. Phytic acid—a natural antioxidant. J. Biol. Chem. 262 (24), 11647–11650.

Grasshoff, K., Kremling, K., Ehrhardt, M., 1999. Methods of Seawater Analysis. Wiley-VCH, Weinheim.

Greene, R.M., Geider, R.J., Falkowski, P.G., 1991. Effect of iron limitation on photosynthesis in a marine diatom. Limnol. Oceanogr. 36 (8), 1772–1782.

Gurney, K.R., Law, R.M., Denning, A.S., Rayner, P.J., Pak, B.C., Baker, D., Bousquet, P., Bruhwiler, L., Chen, Y.H., Ciais, P., Fung, I.Y., Heimann, M., John, J., Maki, T., Maksyutov, S., Peylin, P., Prather, M., Taguchi, S., 2004. Transcom 3 inversion intercomparison: model mean results for the estimation of seasonal carbon sources and sinks. Global Biogeochem. Cycles 18 (1), GB1010. http://dx.doi.org/10.1029/2003GB002111.

Hassler, C.S., Schoemann, V., 2009. Bioavailability of organically bound Fe to model phytoplankton of the Southern Ocean. Biogeosciences 6 (10), 2281–2296.

Hassler, C.S., Schoemann, V., Nichols, C.M., Butler, E.C.V., Boyd, P.W., 2011. Saccharides enhance iron bioavailability to Southern Ocean phytoplankton. Proc. Natl. Acad. Sci. USA 108 (3), 1076–1081.

Hiscock, M.R., Lance, V.P., Apprill, A.M., Bidigare, R.R., Johnson, Z.I., Mitchell, B.G., Smith, W.O., Barber, R.T., 2008. Photosynthetic quantum yield increases are an essential component of the Southern Ocean phytoplankton response to iron. Proc. Natl. Acad. Sci. USA 105 (12), 4775–4780.

Holm-Hansen, O., Lorenzen, C.J., Holmes, R.W., Strickland, J.D.H., 1965. Fluormetric determination of chlorophyll. ICES J. Mar. Sci. 30 (1), 3–15.

Hutchins, D.A., Hare, C.E., Weaver, R.S., Zhang, Y., Firme, G.F., DiTullio, G.R., Alm, M.B., Riseman, S.F., Maucher, J.M., Geesey, M.E., Trick, C.G., Smith, G.J., Rue, E.L., Conn, J., Bruland, K.W., 2002. Phytoplankton iron limitation in the Humboldt current and Peru upwelling. Limnol. Oceanogr. 47 (4), 997–1011.

Hutchins, D.A., Franck, V.M., Brzezinski, M.A., Bruland, K.W., 1999. Inducing phytoplankton iron limitation in iron-replete coastal waters with a strong chelating ligand. Limnol. Oceanogr. 44, 1009–1018.

Keller-Schierlein, W., Mertens, V., Prelog, V., Walser, A., 1965. Stoffwechselprodukte von Actinomyceten. Die Ferrioxamine A1, A2 und D2. Helv. Chim. Acta 48, 710–722.

Kolber, Z.S., et al., 1994. Iron limitation of phytoplankton photosynthesis in the equatorial Pacific Ocean. Nature 371, 145–149.

Kuma, K., Tanaka, J., Matsunaga, K., Matsunaga, K., 2000. Effect of hydroxamate ferrisiderophore complex (ferrichrome) on iron uptake and growth of a coastal diatom, *Chaetoceros sociale*. Limnol. Oceanogr. 45 (6), 1235–1244.

Maldonado, M.T., Strzepek, R.F., Sander, S., Boyd, P.W., 2005. Acquisition of iron bound to strong organic complexes, with different Fe binding groups and photochemical reactivities, by plankton communities in Fe-limited subantarctic waters. Global Biogeochem. Cycles 19 (4).

Martin, J.H., Fitzwater, S.E., 1988. Iron deficiency limits phytoplankton growth in the north-east Pacific subarctic. Nature 331 (28 January 1988), 341–343.

Milligan, A.J., Harrison, P.J., 2000. Effects of non-steady state iron limitation on nitrogen assimilatory enzymes in the marine diatom *Thalassiosira weissflogii* (Bacillariophyceae). J. Phycol. 36, 78–86.

Moline, M.A., Prezelin, B.B., 1997. High resolution time-series data for 1991/1992 primary production and related parameters at a Palmer LTER coastal site: implications for modeling carbon fixation in the Southern Ocean. Polar Biol. 17 (1), 39–53.

Moore, C.M., Mills, M.M., Achterberg, E.P., Geider, R.J., LaRoche, J., Lucas, M.I., McDonagh, E.L., Pan, X., Poulton, A.J., Rijkenberg, M.J.A., Suggett, D.J., Ussher, S.J., Woodward, E.M.S., 2009. Large-scale distribution of Atlantic nitrogen fixation controlled by iron availability. Nat. Geosci. 2 (12), 867–871.

Moore, C.M., Mills, M.M., Milne, A., Langlois, R., Achterberg, E.P., Lochte, K., Geider, R.J., La Roche, J., 2006. Iron limits primary productivity during spring bloom development in the central North Atlantic. Global Change Biol. 12 (4), 626–634.

Moore, C.M., Seeyave, S., Hickman, A.E., Allen, J.T., Lucas, M.I., Planquette, H., Pollard, R.T., Poulton, A.J., 2007. Iron-light interactions during the CROZet natural iron bloom and EXport experiment (CROZEX) I: phytoplankton growth and photophysiology. Deep-Sea Res. II 54 (18-20), 2045–2065.

Mueller, G., Raymond, K.N., 1984. Specificity and mechanism of ferrioxamine-mediated iron transport in *Streptomyces pilosus*. J. Bacteriol. 160, 304–312.
Price, N.M., 2005. The elemental stoichiometry and composition of an iron-limited diatom. Limnol. Oceanogr. 50 (4), 1159–1171.
Raven, J.A., 1990. Predictions of Mn and Fe use efficiencies of phototrophic growth as a function of light availability for growth and of C assimilation pathway. New Phycol. 116, 1–18.
Roy, T., Rayner, P., Matear, R., Francey, R., 2003. Southern hemisphere ocean $CO_2$ uptake: reconciling atmospheric and oceanic estimates. Tellus Ser. B—Chem. Phys. Meteorol. 55, 701–710.
Rue, E.L., Bruland, K.W., 1997. The role of organic complexation on ambient iron chemistry in the equatorial Pacific Ocean and the response of a mesoscale iron addition experiment. Limnol. Oceanogr. 42 (5), 901–910.
Sedwick, P.N., DiTullio, G.R., Mackey, D.J., 2000. Iron and manganese in the Ross Sea, Antarctica: seasonal iron limitation in Antarctic shelf waters. J. Geophys. Res.—Oceans 105 (C5), 11321–11336.
Stolte, W., Kraay, G.W., Noordeloos, A.A.M., Riegman, R., 2000. Genetic and physiological variation in pigment composition of Emiliania huxleyi (Prymnesiophyceae) and the potential use of its pigment ratios as a quantitative physiological marker. J. Phycol. 36 (3), 529–539.
Strzepek, R.F., Harrison, P.J., 2004. Photosynthetic architecture differs in coastal and oceanic diatoms. Nature 431 (7009), 689–692.
Suggett, D.J., Moore, C.M., Hickman, A.E., Geider, R.J., 2009. Interpretation of fast repetition rate (FRR) fluorescence: signatures of phytoplankton community structure versus physiological state. Mar. Ecol.—Prog Ser. 376, 1–19.
Sunda, W.G., Huntsman, S., 1997. Interrelated influence of iron, light and cell size on marine phytoplankton growth. Nature 390, 389–392.
Tagliabue, A., Arrigo, K.R., 2005. Iron in the Ross Sea: 1. Impact on CO2 fluxes via variation in phytoplankton functional group and non-Redfield stoichiometry. J. Geophys. Res.—Oceans 110 (C3), C03009. doi:03010.01029/02004JC002531.
Takahashi, T., Sutherland, S.C., Sweeney, C., Poisson, A., Metzl, N., Tilbrook, B., Bates, N., Wanninkhof, R., Feely, R.A., Sabine, C., Olafsson, J., Nojiri, Y., 2002. Global sea-air CO2 flux based on climatological surface ocean pCO(2), and seasonal biological and temperature effects. Deep-Sea Res. II 49 (9-10), 1601–1622.
Thuróczy, C.E., Alderkamp, A.C., Laan, P., Gerringa, L.J.A., de Baar, H.J.W., Mills, M.M., van Dijken, G.L., Arrigo, K.R., 2012. Key role of organic complexation of iron in sustaining phytoplankton blooms in the Pine Island and Amundsen Polynyas (Southern Ocean). Deep-Sea Res. II 71–76, 49–60.
Van Der Merwe, P., Lannuzel, D., Mancuso Nichols, C.A., Meiners, K., Heil, P., Norman, L., Thomas, D.N., Bowie, A.R., 2009. Biogeochemical observations during the winter-spring transition in East Antarctic sea ice: evidence of iron and exopolysaccharide controls. Marine Chemistry 115 (3-4), 163–175.
van Leeuwe, M.A., Stefels, J., 1998. Effects of iron and light stress on the biochemical composition of Antarctic Phaeocystis sp. (Prymnesiophyceae). II. Pigment composition. J. Phycol. 34 (3), 496–503.
Veldhuis, M.J.W., Timmermans, K.R., Croot, P., van der Wagt, B., 2005. Picophytoplankton; a comparative study of their biochemical composition and photosynthetic properties. J. Sea Res. 53 (1-2), 7–24.
Voss, M., Croot, P., Lochte, K., Mills, M.M., Peeken, I., 2004. Patterns of nitrogen fixation along 10°N in the tropical North Atlantic. Geophys. Res. Lett. 31, L23S09. http://dx.doi.org/10.1029/2004GL020127.
Wells, M.L., Trick, C.G., 2004. Controlling iron availability to phytoplankton in iron-replete coastal waters. Mar. Chem. 86, 1–13.
Wells, M.L., 1999. Manipulating iron availability in nearshore waters. Limnol. Oceanogr. 44 (4), 1002–1008.
Wong, C.S., Johnson, K.S., Sutherland, N., Nishioka, J., Timothy, D.A., Robert, M., Takeda, S., 2006. Iron speciation and dynamics during SERIES, a mesoscale iron enrichment experiment in the NE Pacific. Deep-Sea Res. II 53 (20-22), 2075–2094.